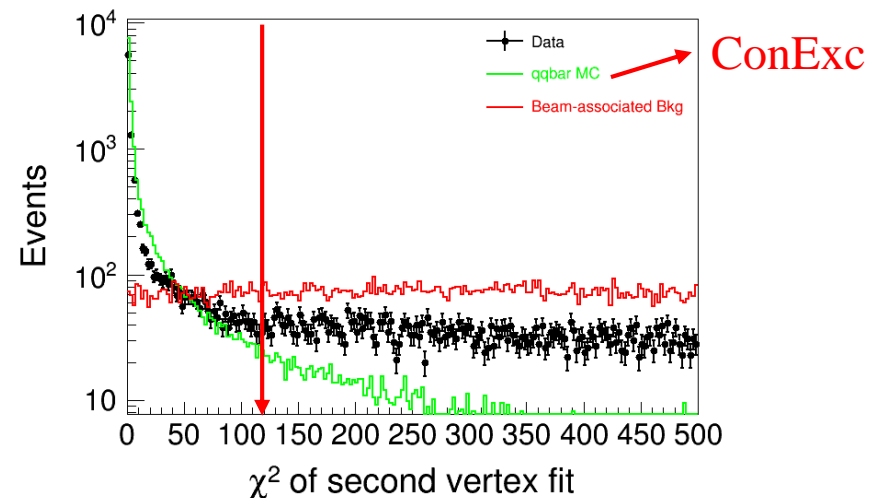
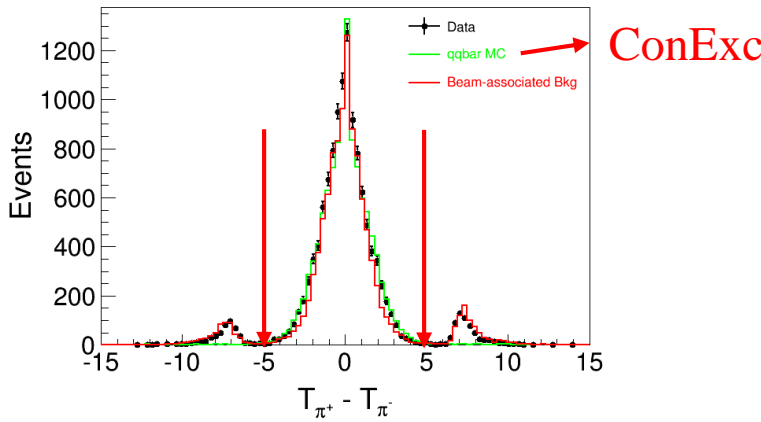


Ks cut criteria

- ✓ Track selection
 - $|V_r| < 10\text{cm}$, $|V_z| < 30\text{cm}$
- ✓ PID: Prob $\pi >$ Prob K and Prob $\pi >$ Prob P
 $N_{\pi^+} \geq 1$ and $N_{\pi^-} \geq 1$
- ✓ Second vertex fitting: $L/\sigma_L > 2.0$



- ✓ Remove the cosmic rays: $|T(\pi^+) - T(\pi^-)| < 5$
- ✓ Remove the beam-associated backgrounds: $\chi^2(\text{second vertex fit}) < 120$

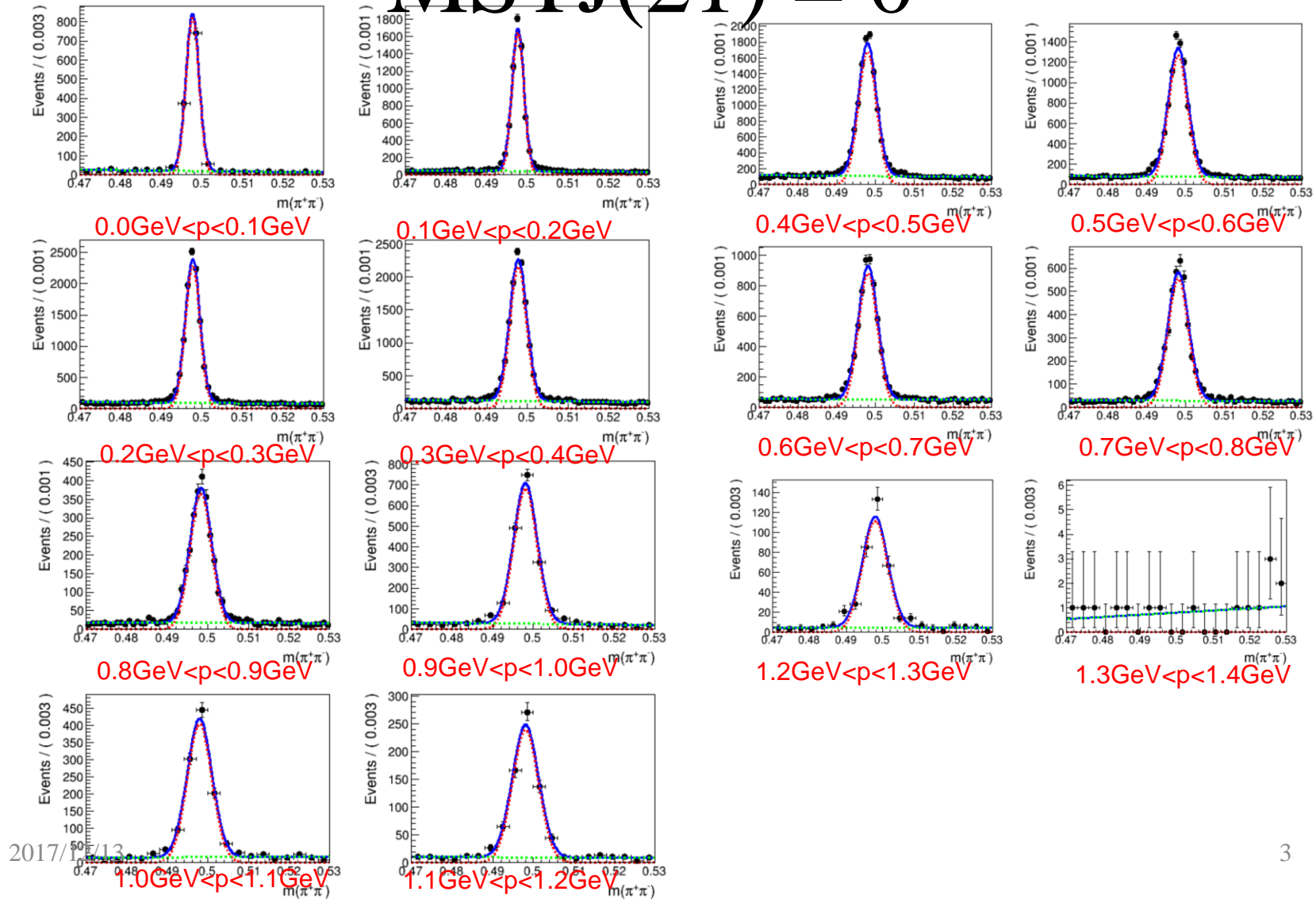
1, Ks efficiency differences

Here, MSTJ(21) = 0

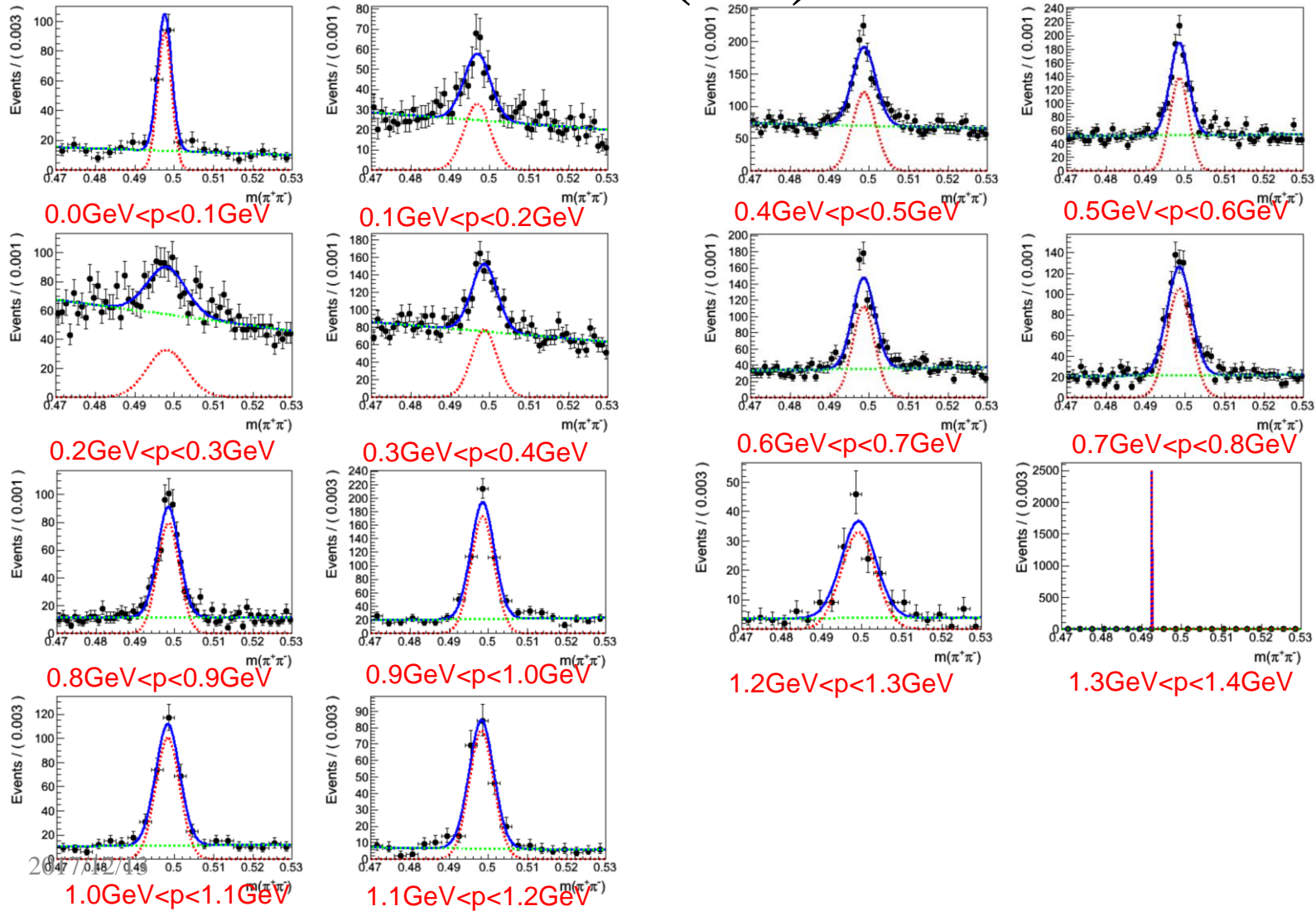
Table 18: K_S^0 efficiencies (%) vary with momentum in different MC models.

p(GeV)	$\varepsilon(K_S^0)$ from ConExc	$\varepsilon(K_S^0)$ from Lundalw(0)	Uncertainty
0.0-0.1	30.3	33.0	-9.1
0.1-0.2	39.8	40.8	-2.4
0.2-0.3	44.3	44.6	-0.6
0.3-0.4	45.3	46.1	-1.9
0.4-0.5	48.2	47.7	0.9
0.5-0.6	45.3	50.6	-11.8
0.6-0.7	43.4	51.7	-19.1
0.7-0.8	44.3	53.9	-21.6
0.8-0.9	49.6	55.6	-12.1
0.9-1.0	55.8	54.3	2.6
1.0-1.1	52.8	54.5	-3.3
1.1-1.2	47.8	49.1	-2.7
1.2-1.3	62.6	52.3	16.4

K_s mass distribution with MSTJ(21) = 0

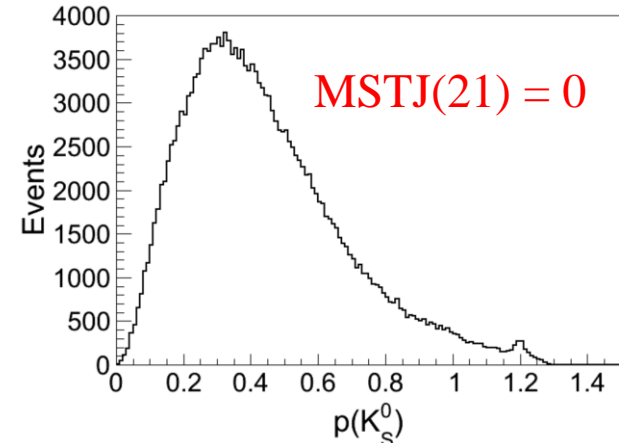
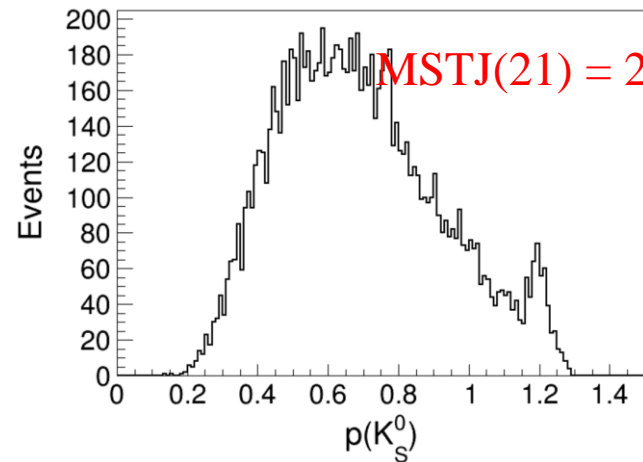


K_s mass distribution with MSTJ(21) = 2

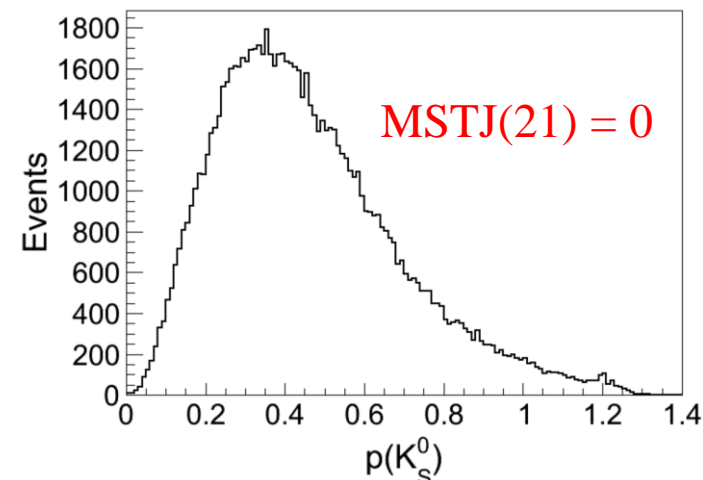
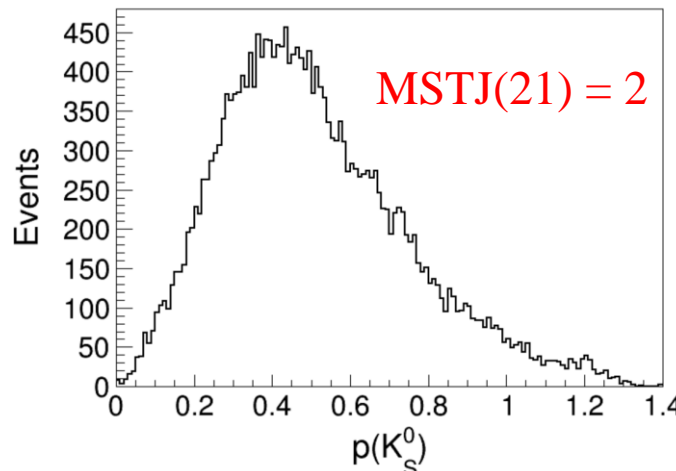


K_s momentum in truth level and detect level

K_s momentum
in truth level:

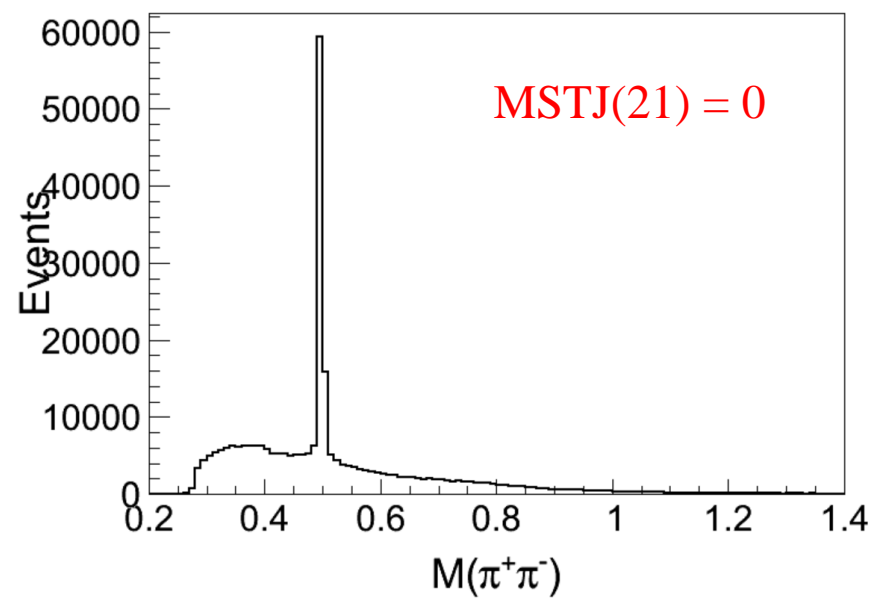
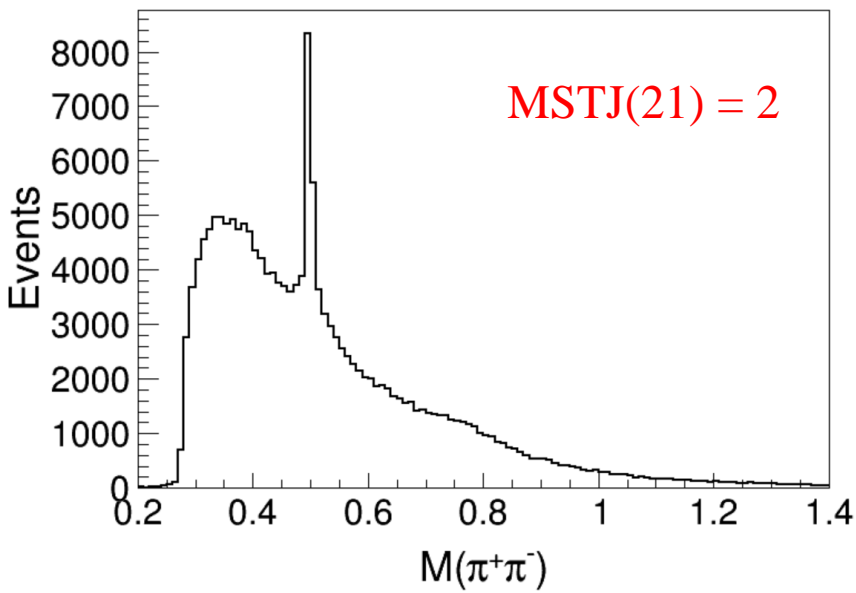


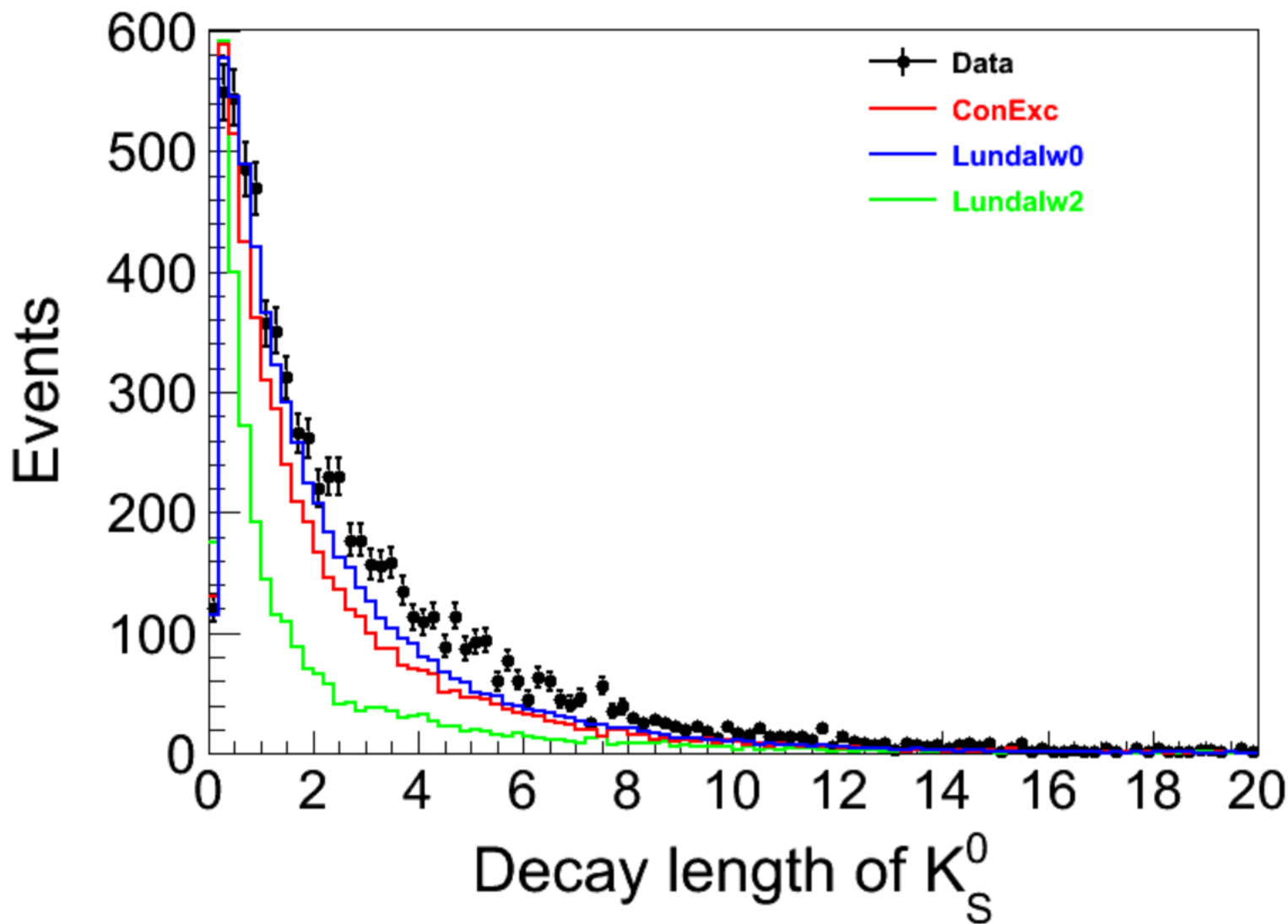
K_s momentum
in detect level:



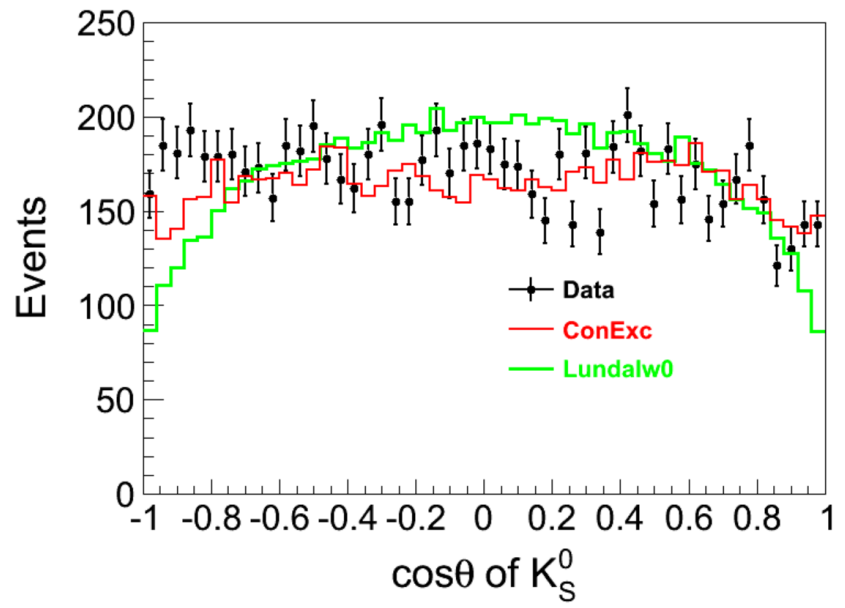
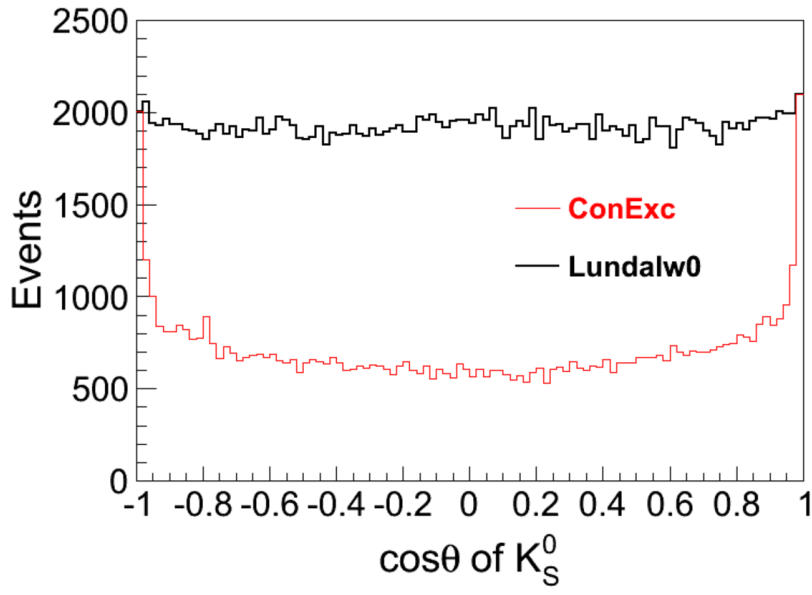
Ks mass in detect level

Ks mass in detect level:

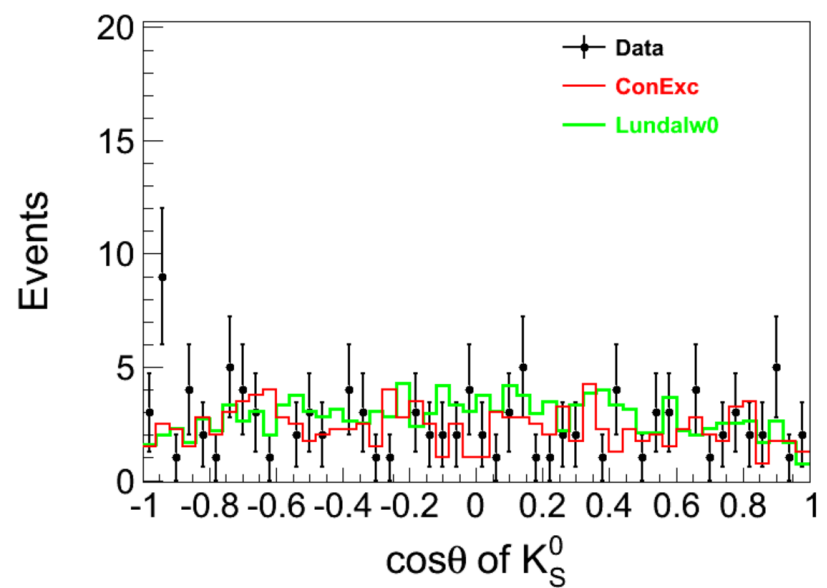
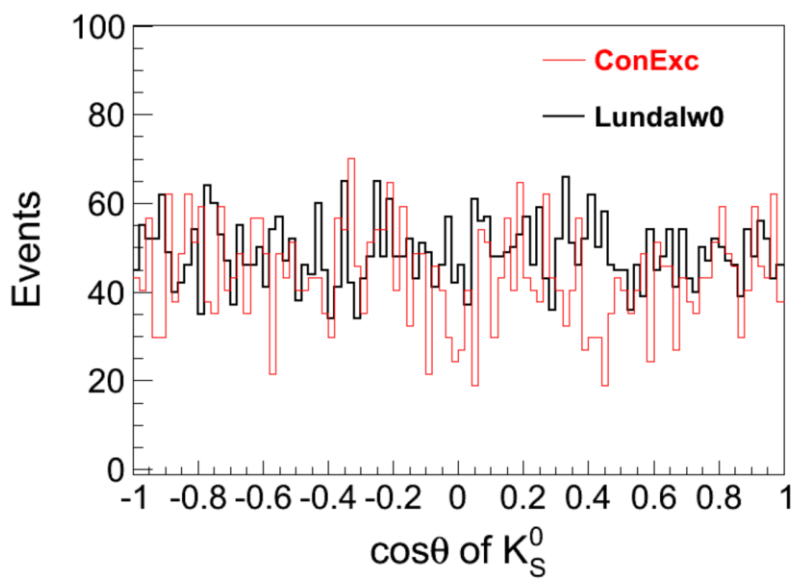




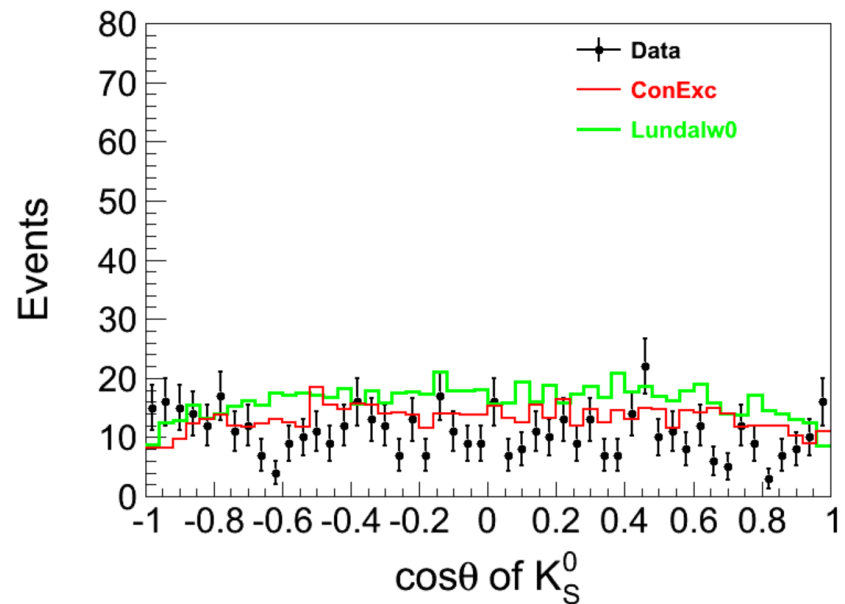
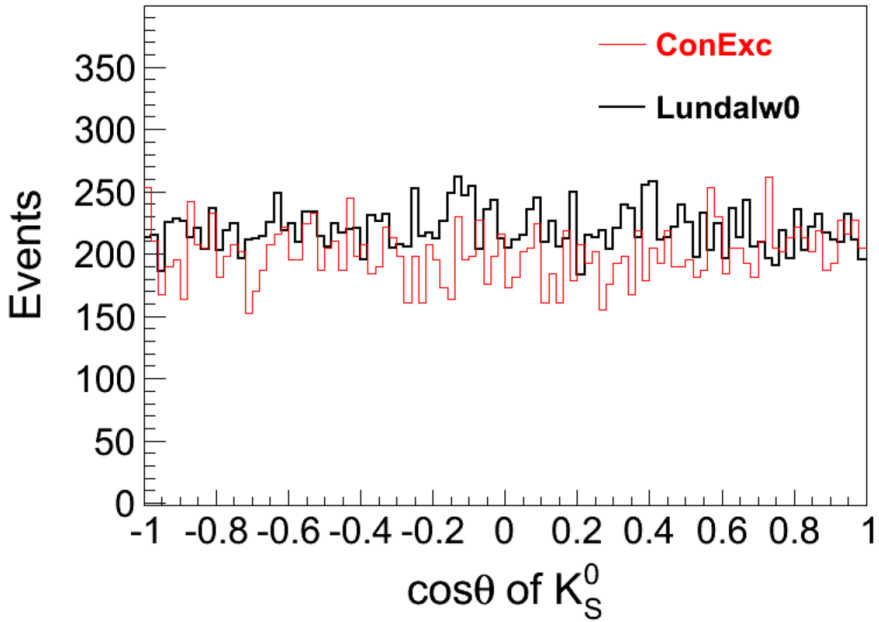
Costheta distribution



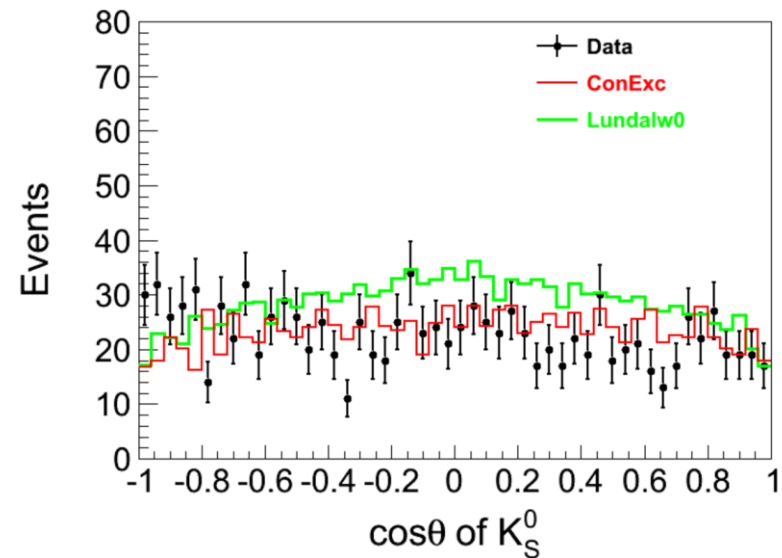
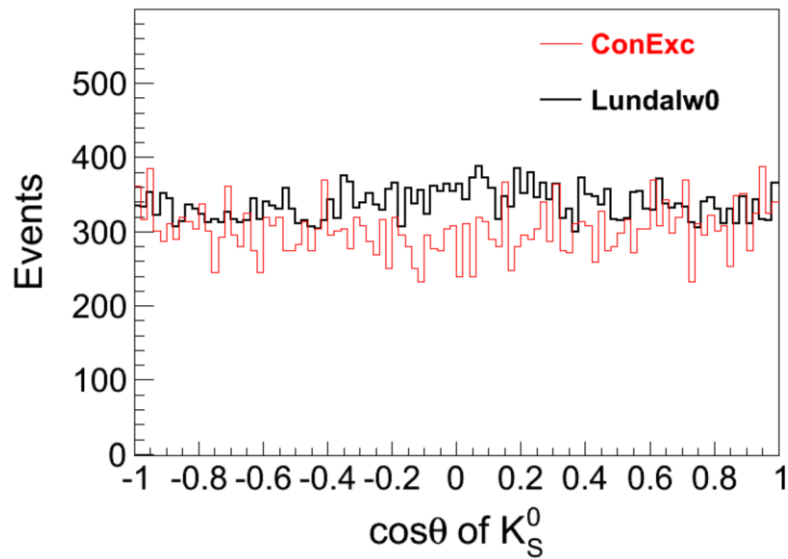
0.0-0.1



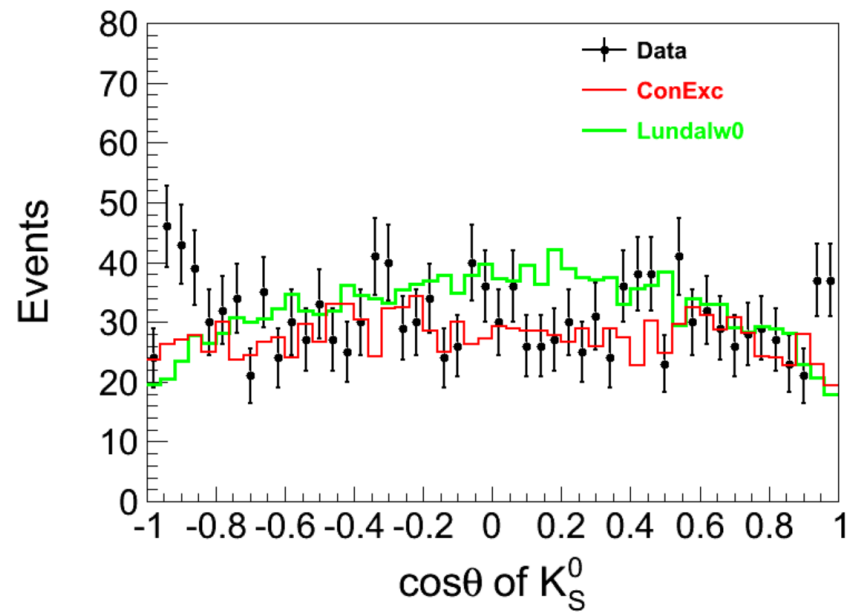
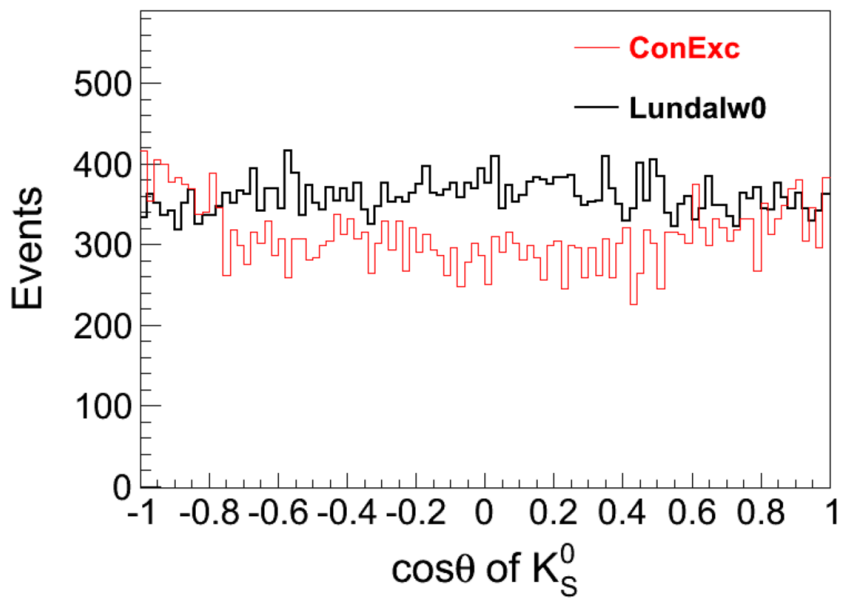
0.1-0.2



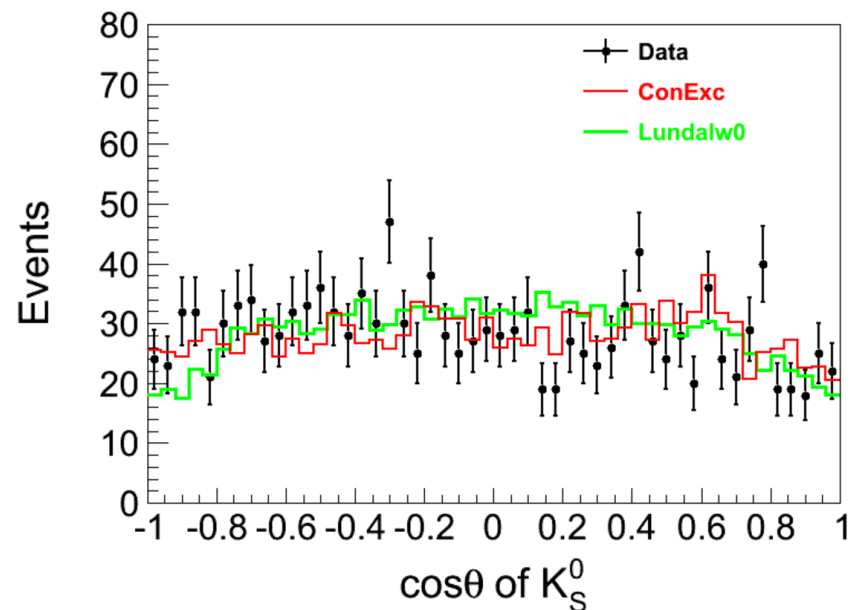
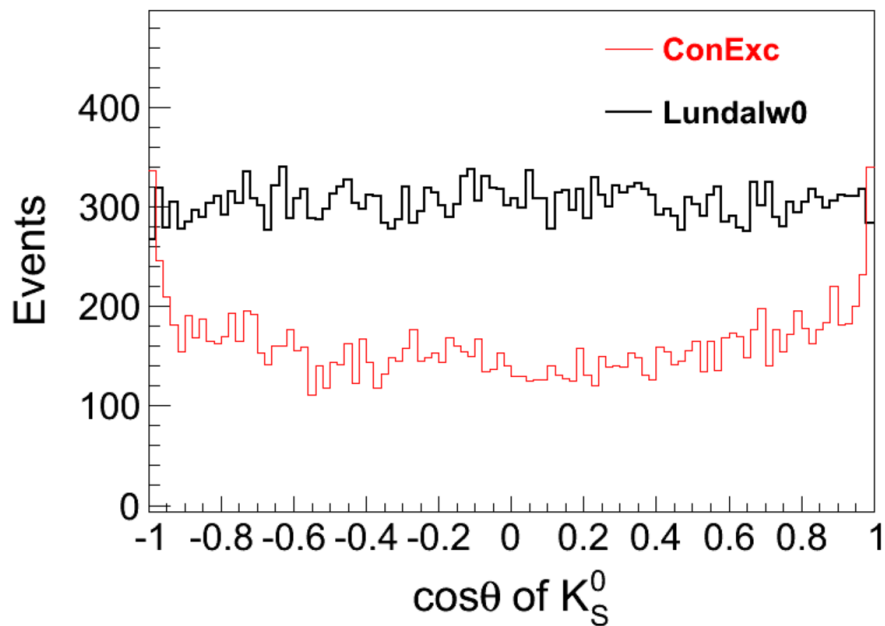
0.2-0.3



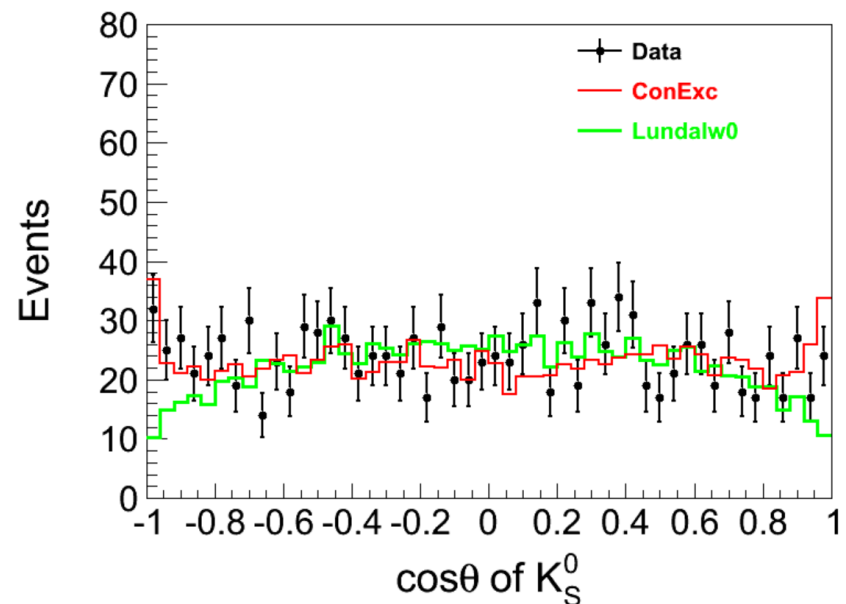
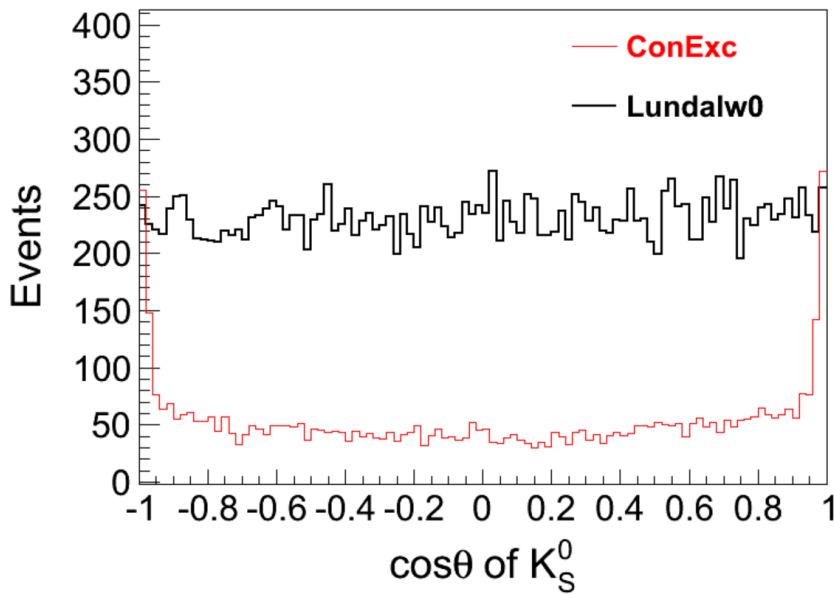
0.3-0.4



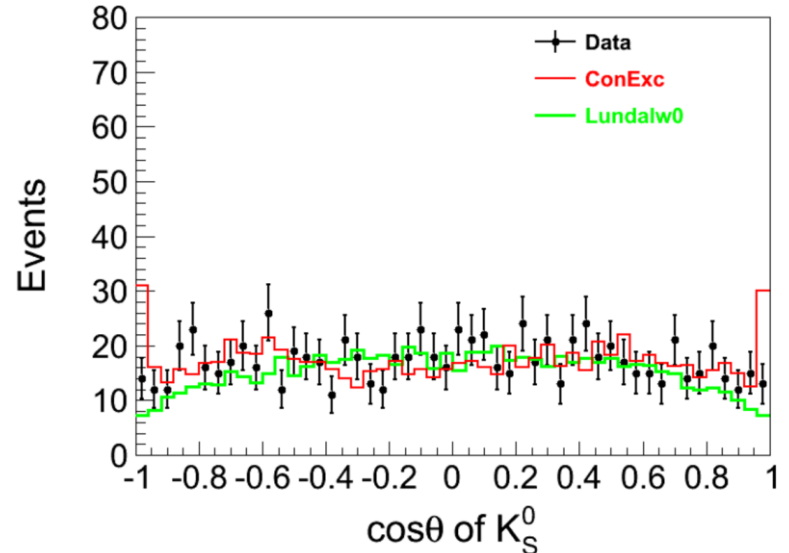
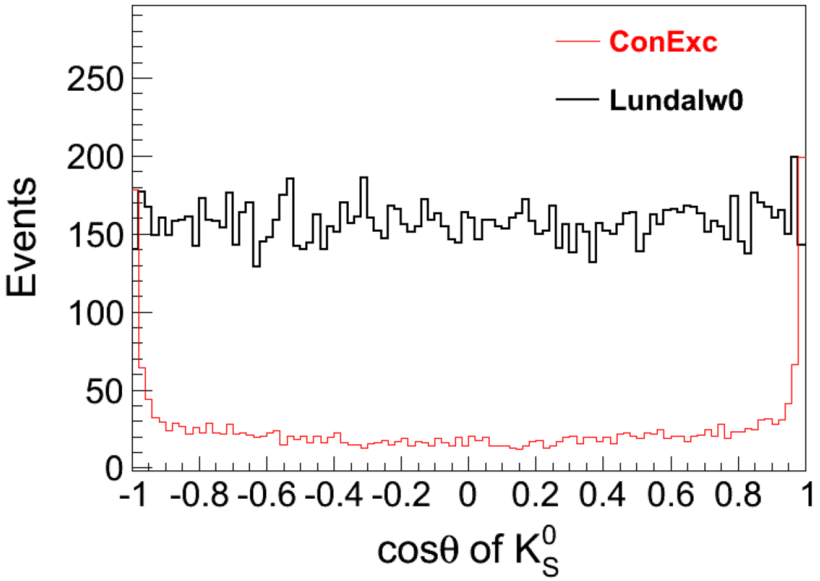
0.4-0.5



0.5-0.6



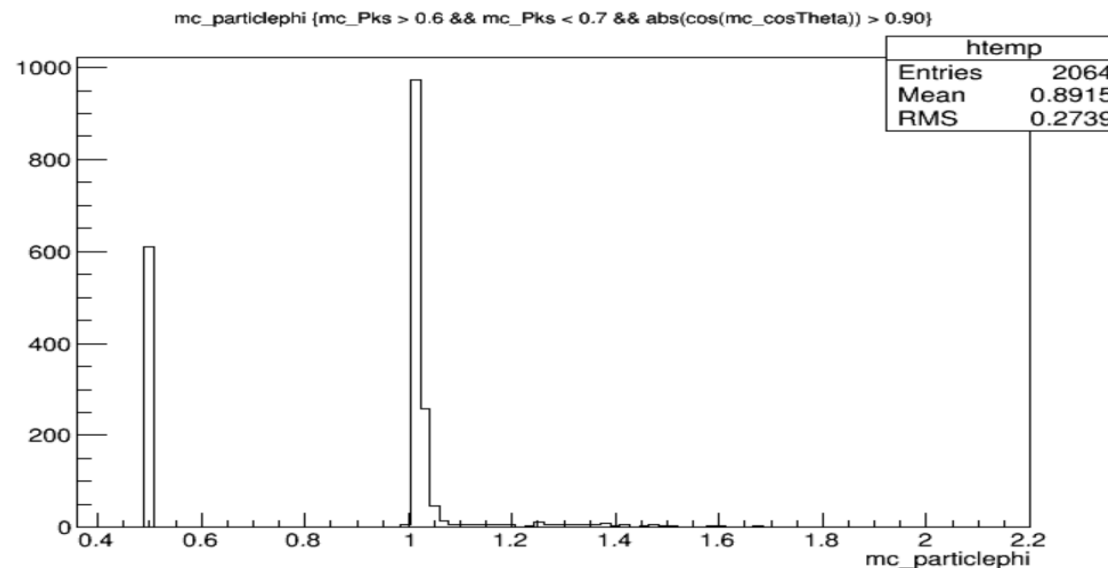
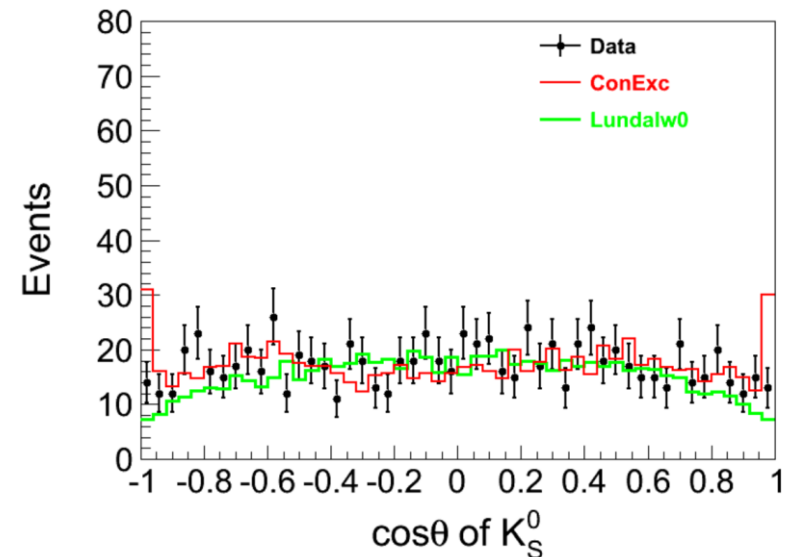
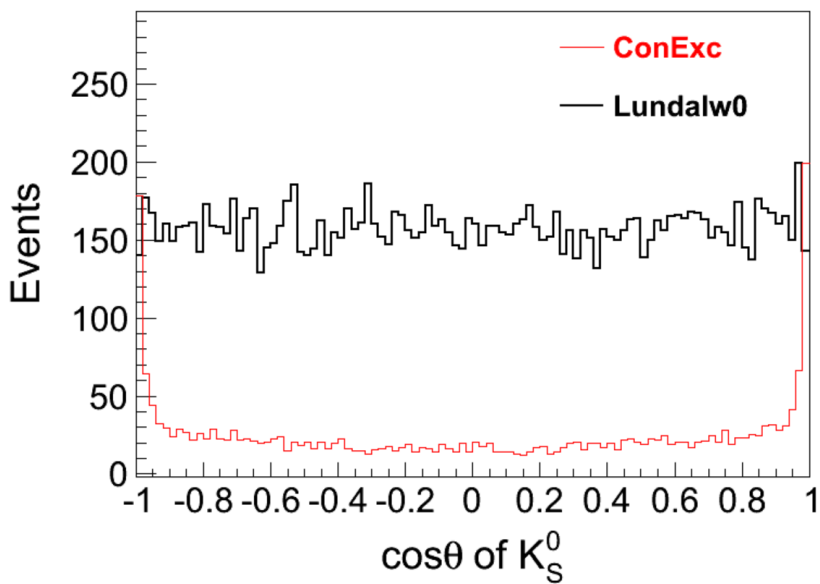
0.6-0.7



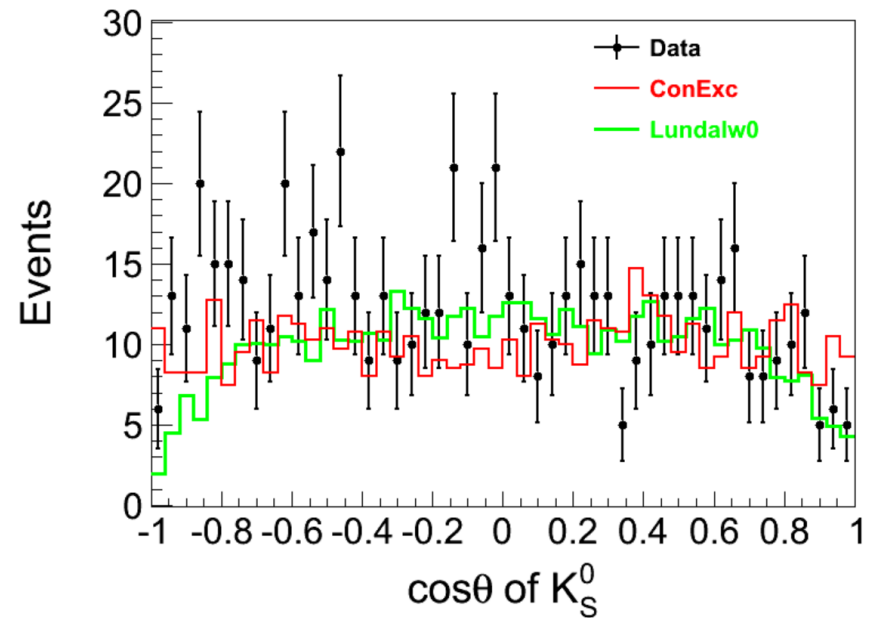
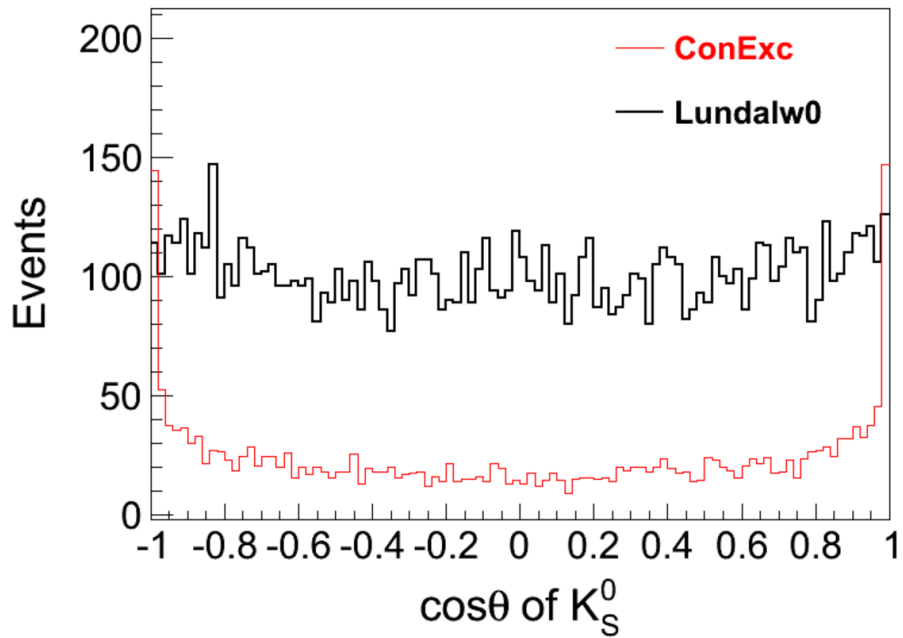
No.	decay chain	final states	iTopo	nEvt	nTot
0	$e^+e^- \rightarrow \gamma K_L K_S, K_S \rightarrow \pi^-\pi^+$	$e^+e^- \rightarrow \gamma\pi^+K_L\pi^-$	5	179	179
1	$e^+e^- \rightarrow \gamma\gamma^*, \gamma^* \rightarrow \pi^-\pi^-\pi^0\pi^+\pi^+\pi^+$	$e^+e^- \rightarrow \gamma\pi^+\pi^+\pi^0\pi^-\pi^-\pi^-$	17	66	245
2	$e^+e^- \rightarrow \pi^-\pi^-\pi^0\pi^+\pi^+$	$e^+e^- \rightarrow \pi^+\pi^+\pi^0\pi^0\pi^-\pi^-$	13	61	306
3	$e^+e^- \rightarrow \gamma\gamma^*, \gamma^* \rightarrow \pi^-\pi^-\pi^-\pi^+\pi^+\pi^+$	$e^+e^- \rightarrow \gamma\pi^+\pi^+\pi^-\pi^-\pi^-$	3	44	350
4	$e^+e^- \rightarrow \gamma\gamma K_L K_S, K_S \rightarrow \pi^-\pi^+$	$e^+e^- \rightarrow \gamma\gamma\pi^+K_L\pi^-$	41	40	390
5	$e^+e^- \rightarrow \pi^-\pi^-\pi^+\pi^+\pi^+$	$e^+e^- \rightarrow \pi^+\pi^+\pi^+\pi^-\pi^-\pi^-$	0	30	420
6	$e^+e^- \rightarrow \pi^-\pi^-\gamma\pi^+\pi^+$	$e^+e^- \rightarrow \gamma\pi^+\pi^-\pi^-\pi^-$	54	21	441
7	$e^+e^- \rightarrow \pi^-\gamma\pi^0\pi^+$	$e^+e^- \rightarrow \gamma\pi^+\pi^0\pi^-$	38	16	457
8	$e^+e^- \rightarrow \pi^-\gamma\pi^0\pi^0\pi^+$	$e^+e^- \rightarrow \gamma\pi^+\pi^0\pi^-\pi^-$	29	11	468
9	$e^+e^- \rightarrow a_1^-\pi^+a_1^0, a_1^- \rightarrow \pi^-\rho^0, a_1^0 \rightarrow \pi^-\rho^+, \rho^+ \rightarrow \pi^0\pi^+, \rho^0 \rightarrow \pi^-\pi^+$	$e^+e^- \rightarrow \pi^+\pi^+\pi^+\pi^0\pi^-\pi^-\pi^-$	16	8	476
10	$e^+e^- \rightarrow K^-\pi^-\pi^0\pi^+K^+$	$e^+e^- \rightarrow K^+\pi^+\pi^0\pi^-K^-$	60	8	484
11	$e^+e^- \rightarrow \gamma\gamma^*, \gamma^* \rightarrow \pi^-\pi^-K_SK^+, K_S \rightarrow \pi^-\pi^+$	$e^+e^- \rightarrow \gamma K^+\pi^+\pi^-\pi^-$	117	7	491
12	$e^+e^- \rightarrow a_1^-K_SK^+, a_1^- \rightarrow \pi^-\rho^0, K_S \rightarrow \pi^-\pi^+, \rho^0 \rightarrow \pi^-\pi^+$	$e^+e^- \rightarrow K^+\pi^+\pi^+\pi^-\pi^-$	55	6	497
13	$e^+e^- \rightarrow \gamma\gamma^*, \gamma^* \rightarrow \pi^-\pi^-\pi^0\pi^+\pi^+$	$e^+e^- \rightarrow \gamma\pi^+\pi^+\pi^0\pi^-\pi^-$	140	6	503
14	$e^+e^- \rightarrow \pi^-\pi^-\pi^+\pi^+\eta, \eta \rightarrow \gamma\gamma$	$e^+e^- \rightarrow \gamma\gamma\pi^+\pi^-\pi^-$	209	6	509
15	$e^+e^- \rightarrow \pi^-\pi^-\pi^0\pi^+\pi^+$	$e^+e^- \rightarrow \pi^+\pi^+\pi^+\pi^-\pi^-$	63	5	514
16	$e^+e^- \rightarrow K^-K_S a_1^-, K_S \rightarrow \pi^-\pi^+, a_1^- \rightarrow \rho^0\pi^+, \rho^0 \rightarrow \pi^-\pi^+$	$e^+e^- \rightarrow \pi^+\pi^+\pi^+\pi^-\pi^-K^-$	76	5	519
17	$e^+e^- \rightarrow \gamma\gamma^*, \gamma^* \rightarrow \pi^-\pi^-\pi^+\pi^+\eta, \eta \rightarrow \pi^-\pi^0\pi^+$	$e^+e^- \rightarrow \gamma\pi^+\pi^+\pi^+\pi^0\pi^-\pi^-$	23	5	524
18	$e^+e^- \rightarrow K_L K_S a_1^0, K_S \rightarrow \pi^-\pi^+, a_1^0 \rightarrow \pi^-\rho^+, \rho^+ \rightarrow \pi^0\pi^+$	$e^+e^- \rightarrow \pi^+\pi^+K_L\pi^0\pi^-\pi^-$	36	5	529
19	$e^+e^- \rightarrow \pi^-\pi^-\pi^+\pi^+\eta, \eta \rightarrow \pi^-\pi^0\pi^+$	$e^+e^- \rightarrow \pi^+\pi^+\pi^+\pi^0\pi^-\pi^-$	42	5	534

Table 1: The possible background channels extracted from Inclusive MC sample

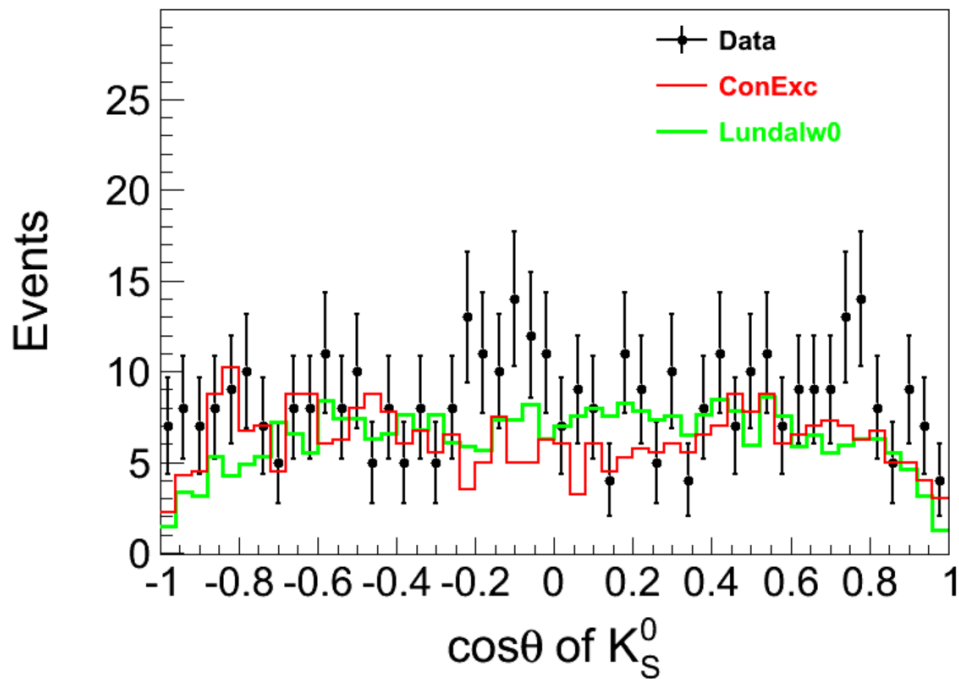
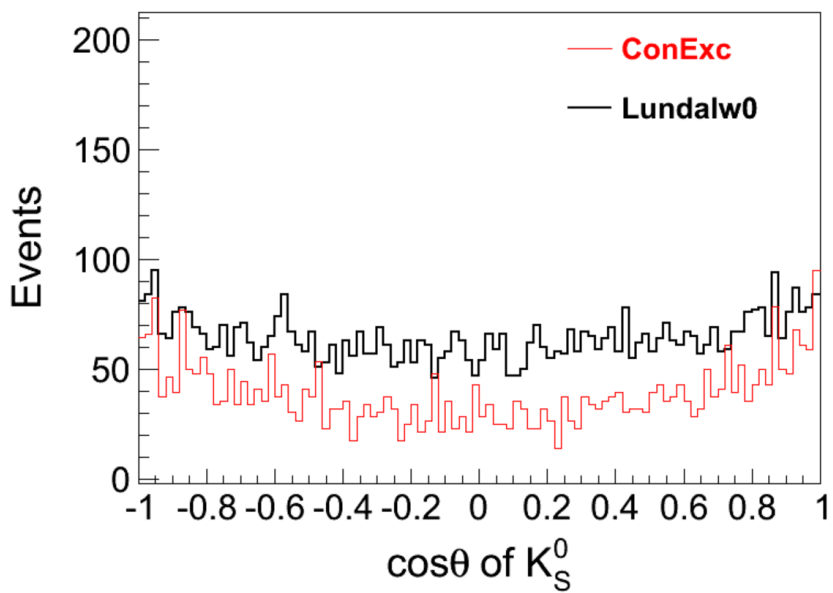
0.6-0.7



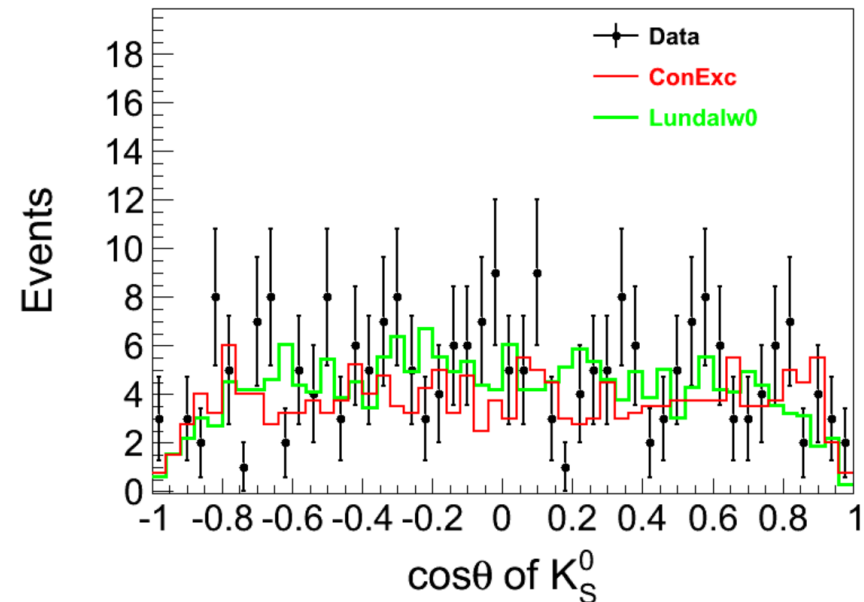
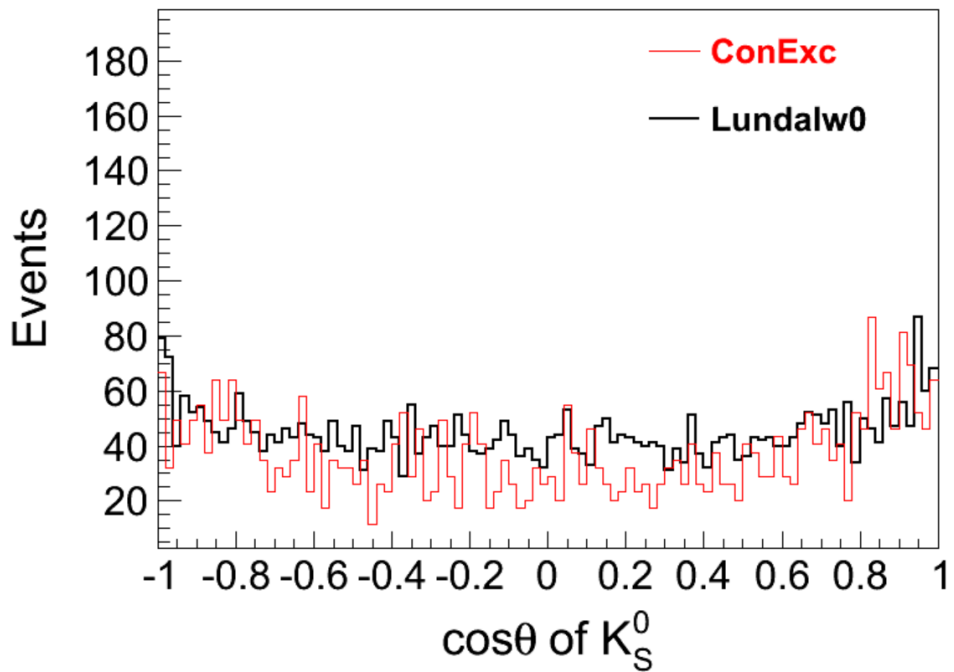
0.7-0.8



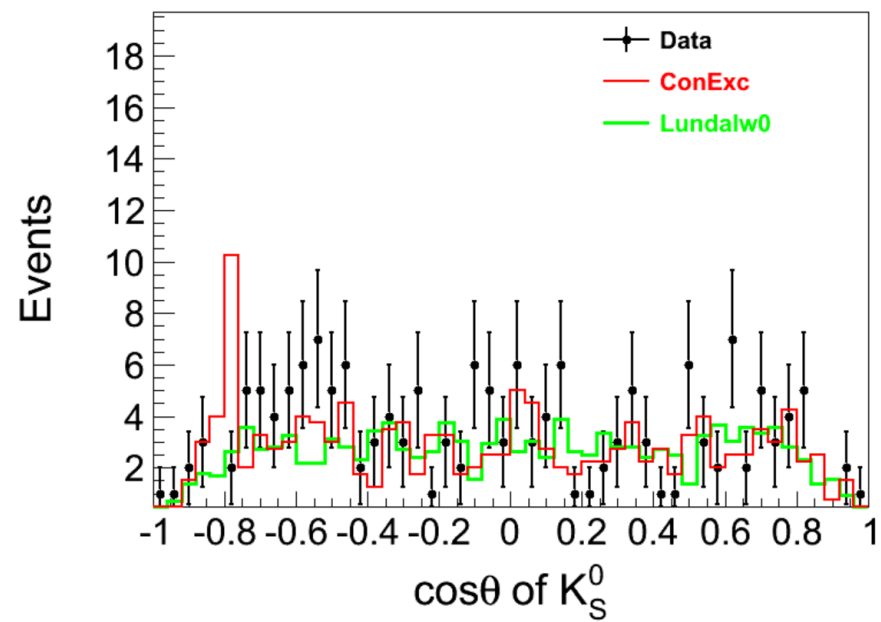
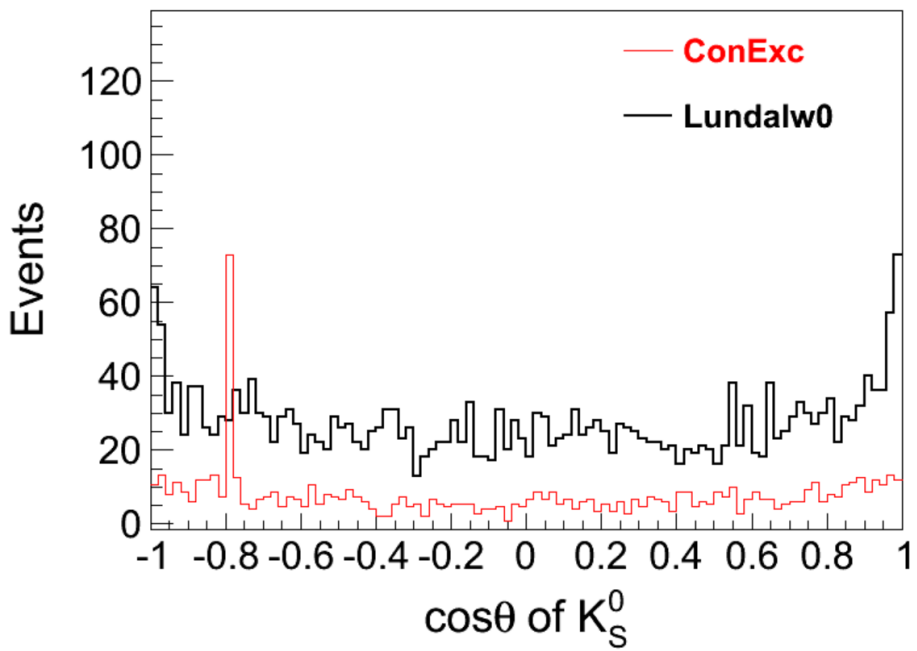
0.8-0.9



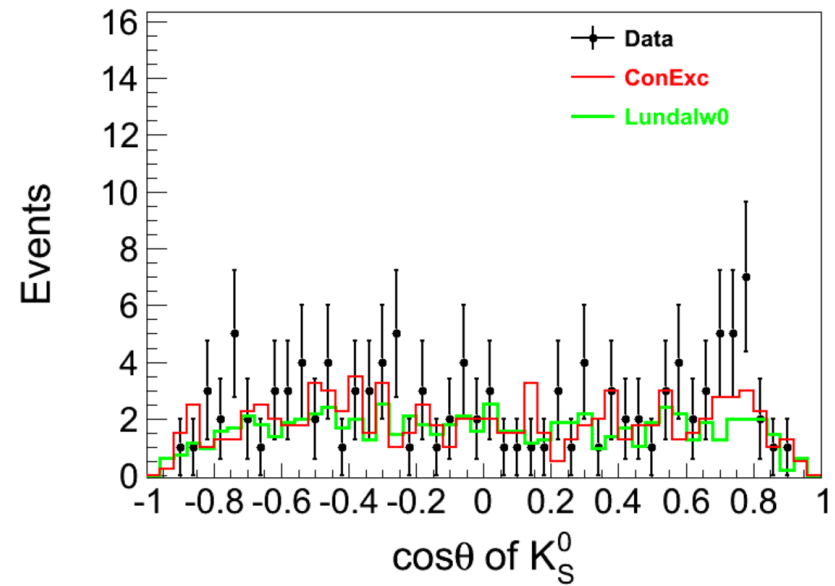
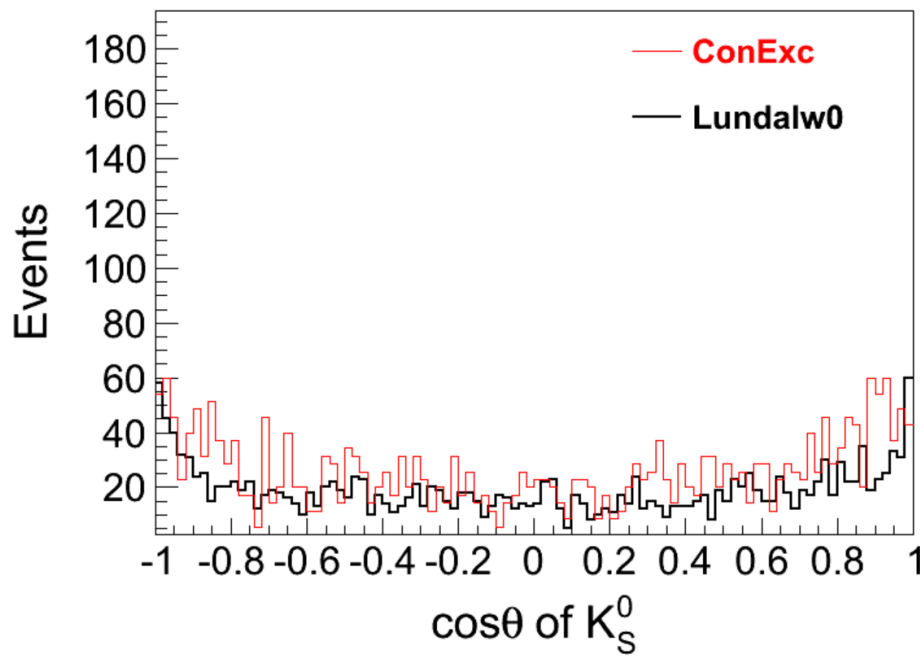
0.9-1.0



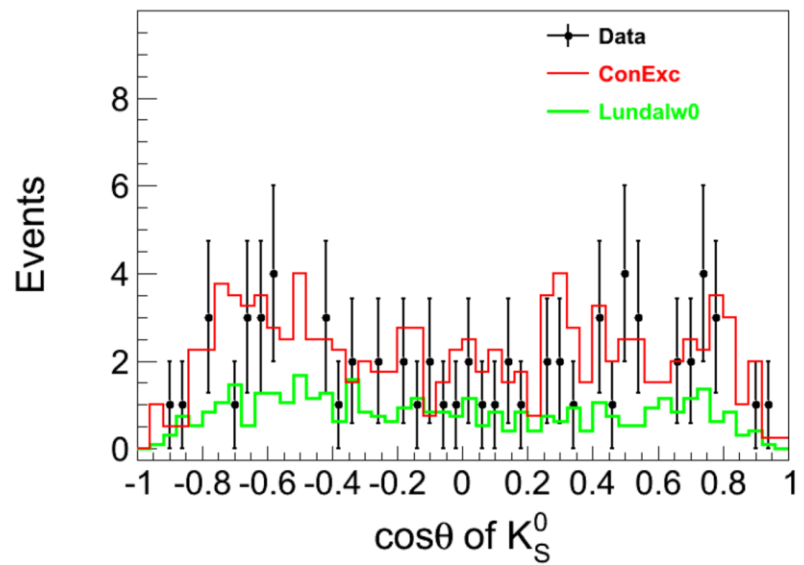
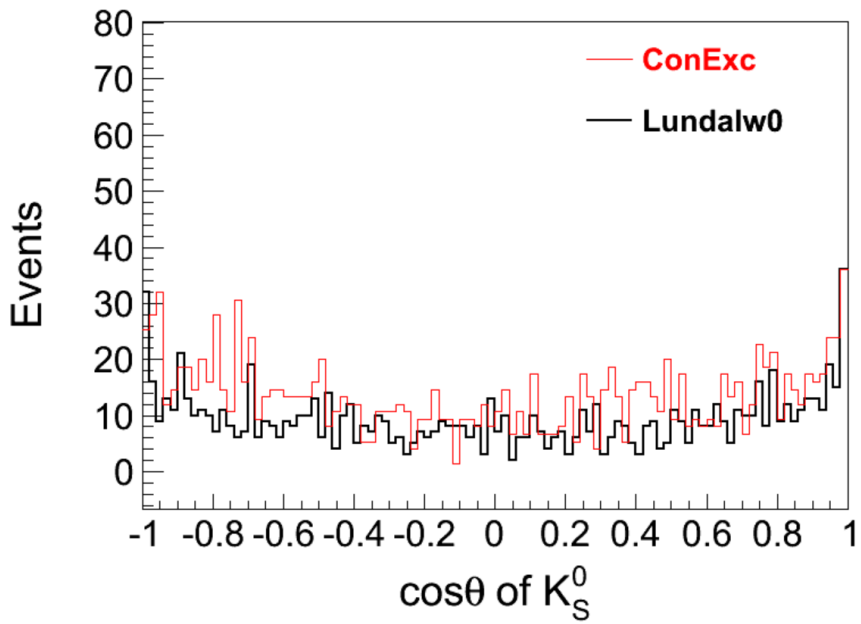
1.0-1.1



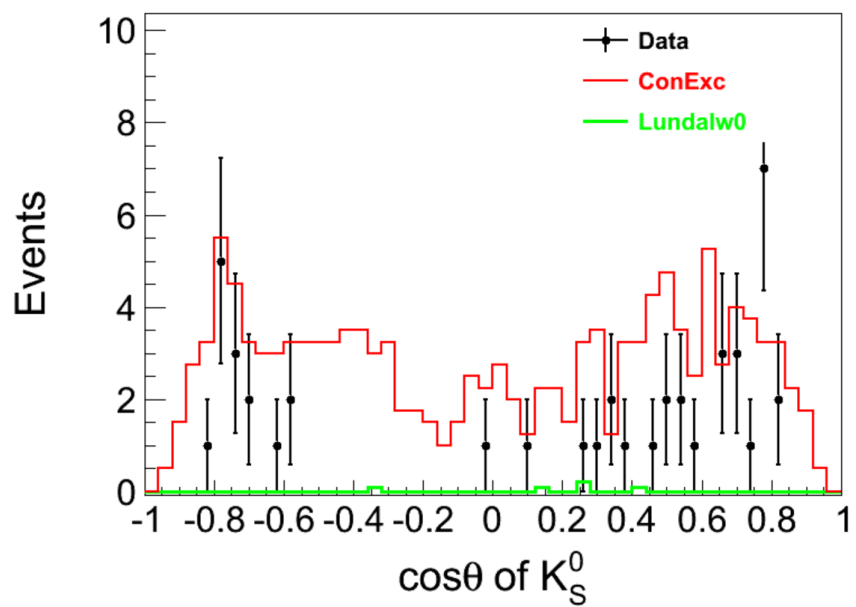
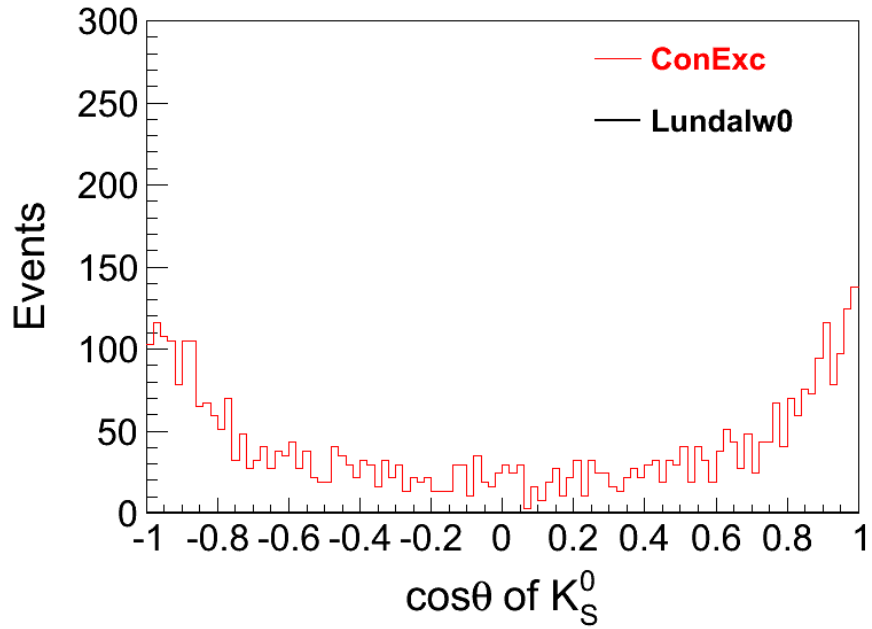
1.1-1.2



1.2-1.3



1.3-1.4



2, Hadron efficiency differences

- Hadronic event selection efficiency:

74.2% (Here, the generator is Lundalw, and **MSTJ(21) = 2**, Gao zhen's efficiency is 72.7%)

82.9% (Here, the generator is Lundalw, and **MSTJ(21) = 0**)

72.8% (Here, the generator is ConExc, and Gao Zhen's efficiency is 72.7%)

Cut flow for hadronic event selection:

Table 19: Hadron efficiencies (%) using different Lundalw parameters.

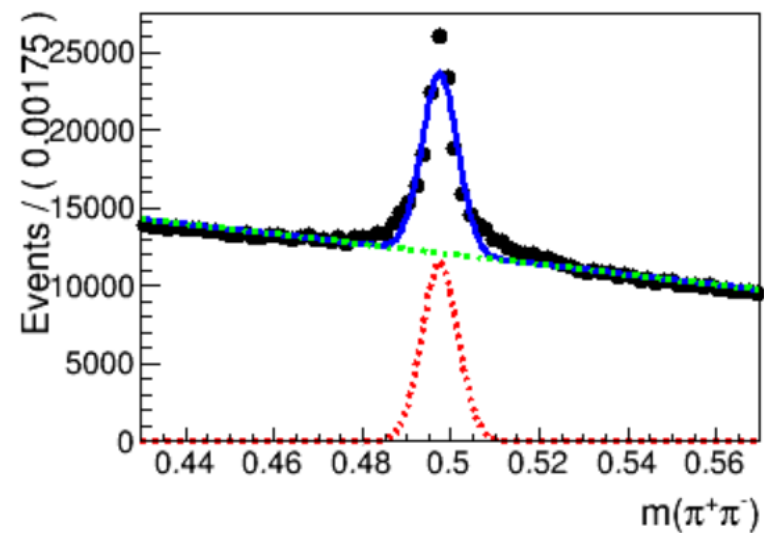
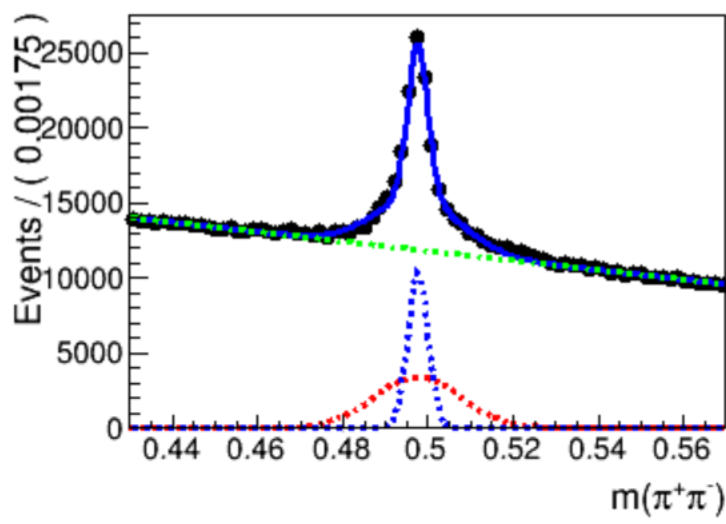
Cut criteria	ConExc		Lundalw(0)		Lundalw(2)		ϵ diff
	Events	$\epsilon(hadron)$	Events	$\epsilon(hadron)$	Events	$\epsilon(hadron)$	
Total events	200000	-	200000	-	200000	-	-
$N_{good} \geq 1$ (No cut)	190099	95.05	195206	97.60	185006	92.50	5.5
$ \theta_1 + \theta_2 - 180^\circ < 10^\circ$ and $E > 0.65 * E_{beam}$	199937	99.97	199983	99.99	199960	99.98	0.01
$N_{good} \geq 2$	164894	82.47	180048	90.03	162542	81.29	10.8
$N_{good} = 2$ $ \theta_1 + \theta_2 - 180^\circ < 15^\circ$ and $ \phi_1 - \phi_2 - 180^\circ < 10^\circ$	54850	-	44676	-	40356	-	-
$N_{Isolated} \geq 2$	52805	96.27	43032	96.32	39061	97.15	-0.9
	38316	72.56	33792	78.53	28955	71.75	9.4
	148360	89.97	169164	93.95	151141	92.75	1.3
$N_{good} = 3$ $ \theta_1 + \theta_2 - 180^\circ < 15^\circ$ and $ \phi_1 - \phi_2 - 180^\circ < 10^\circ$	38313	-	46034	-	39084	-	-
$N_{eop} > 1$	36892	96.29	44232	96.09	37548	96.03	-0.1
$N_{ProbE} > 1$	35959	97.45	43096	97.43	36610	93.67	4.0
	35526	98.80	42710	99.10	36259	99.04	0.1
	145573	98.12	165840	98.04	148316	98.13	-0.1
Finally Efficiency	145573	72.79	165840	82.92	148316	74.16	11.8

Table 22: K_S^0 efficiencies (%) vary with momentum in different MC models.

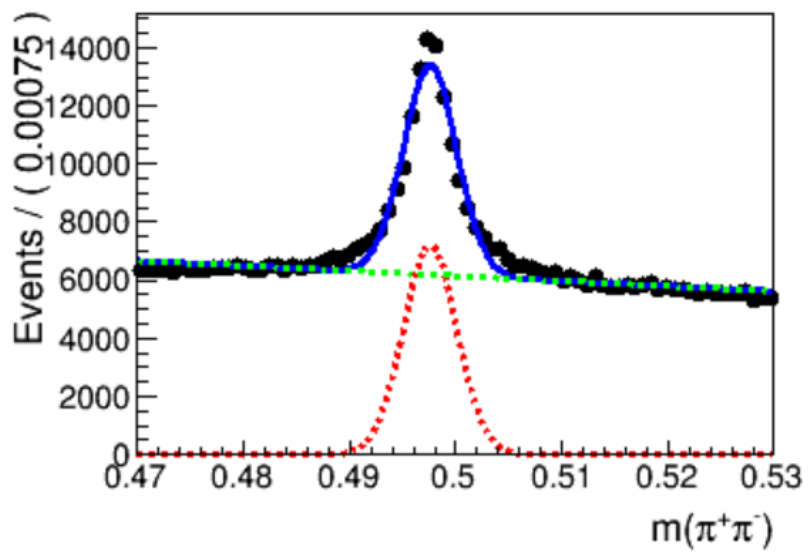
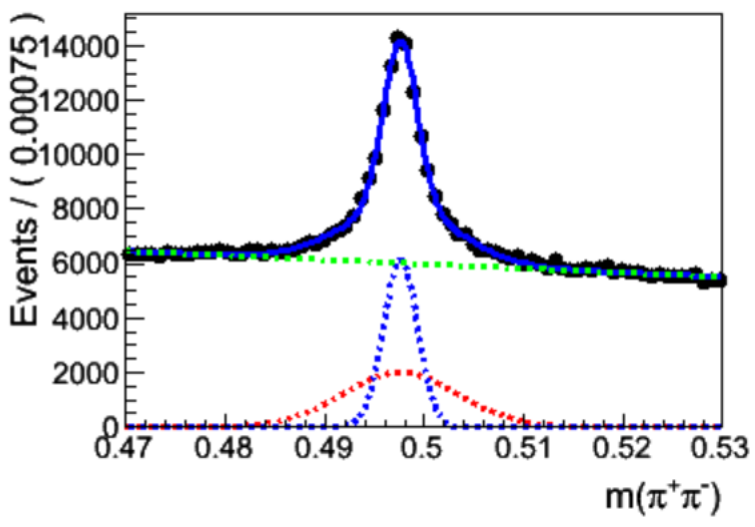
p(GeV)	$\varepsilon(K_S^0)$ ConExc	$\varepsilon(K_S^0)$ Lundalw(0)	$\varepsilon(K_S^0)$ Lundalw(2)S	Lundalw(2)D
0.0-0.1	64.2 ± 3.3	68.6 ± 1.8	46.4 ± 2.0	72.8 ± 21.9
0.1-0.2	62.8 ± 1.8	61.3 ± 0.9	48.3 ± 1.1	75.2 ± 3.3
0.2-0.3	55.9 ± 1.7	56.9 ± 0.8	43.5 ± 1.0	53.9 ± 2.3
0.3-0.4	55.2 ± 2.3	51.4 ± 0.9	46.6 ± 1.1	67.0 ± 2.5
0.4-0.5	56.5 ± 3.0	52.1 ± 1.2	57.4 ± 1.1	73.6 ± 3.3
0.5-0.6	46.8 ± 3.5	47.7 ± 1.6	53.5 ± 1.3	88.1 ± 6.9
0.6-0.7	45.8 ± 3.3	45.5 ± 2.4	53.4 ± 1.6	79.0 ± 18.3
0.7-0.8	34.8 ± 15.1	43.9 ± 3.0	66.5 ± 1.9	109.1 ± 25.4
0.8-0.9	38.5 ± 5.9	45.9 ± 4.3	51.8 ± 2.5	71.1 ± 6.3
0.9-1.0	24.7 ± 6.5	41.2 ± 5.2	51.3 ± 2.7	68.8 ± 6.9
1.0-1.1	22.0 ± 6.1	35.1 ± 7.8	44.7 ± 2.9	67.9 ± 13.5
1.1-1.2	22.6 ± 5.7	22.9 ± 4.3	48.2 ± 3.1	69.2 ± 10.7
1.2-1.3	30.2 ± 4.6	25.1 ± 7.2	50.3 ± 4.9	84.7 ± 18.4

$$\begin{aligned} \text{Lundalw(0)s} &= 61209 \pm 500 & \text{Lundalw(2)s} &= 67316.3 \pm 558 \\ \text{Lundalw(0)d} &= 74132 \pm 1789 & \text{Lundalw(2)d} &= 85500 \pm 1408 \end{aligned}$$

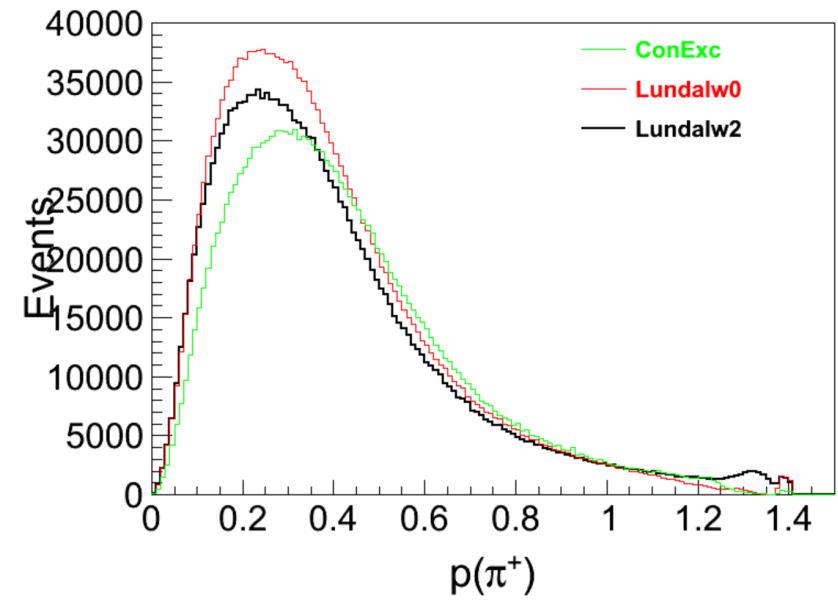
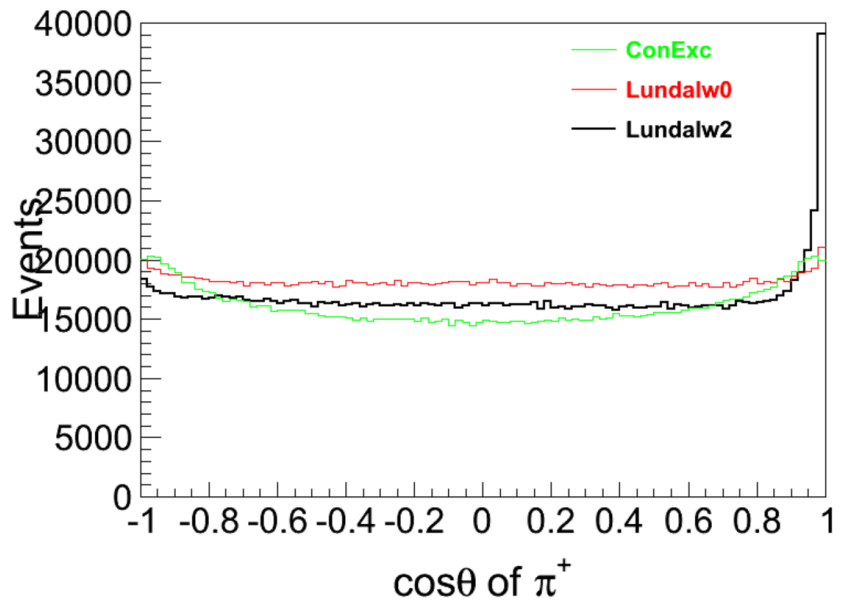
Lundalw2 (Total fit)



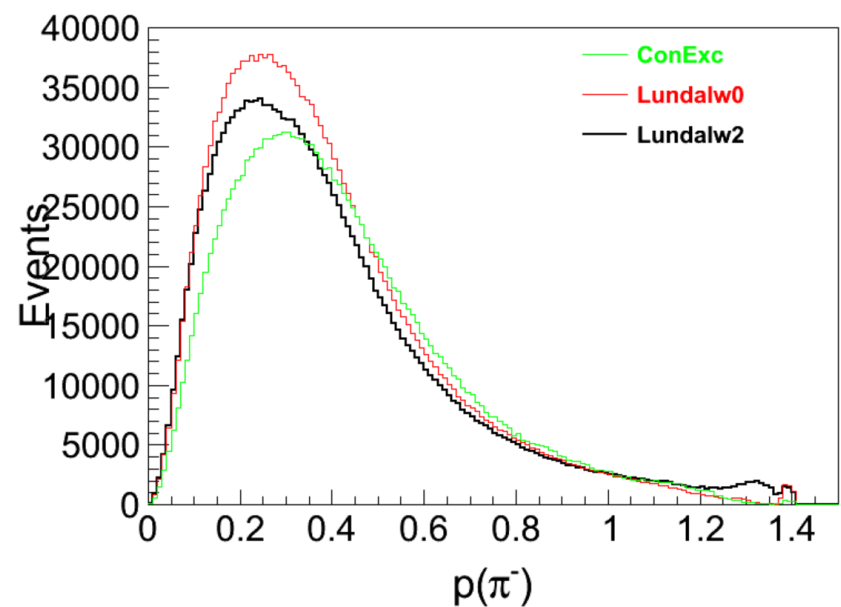
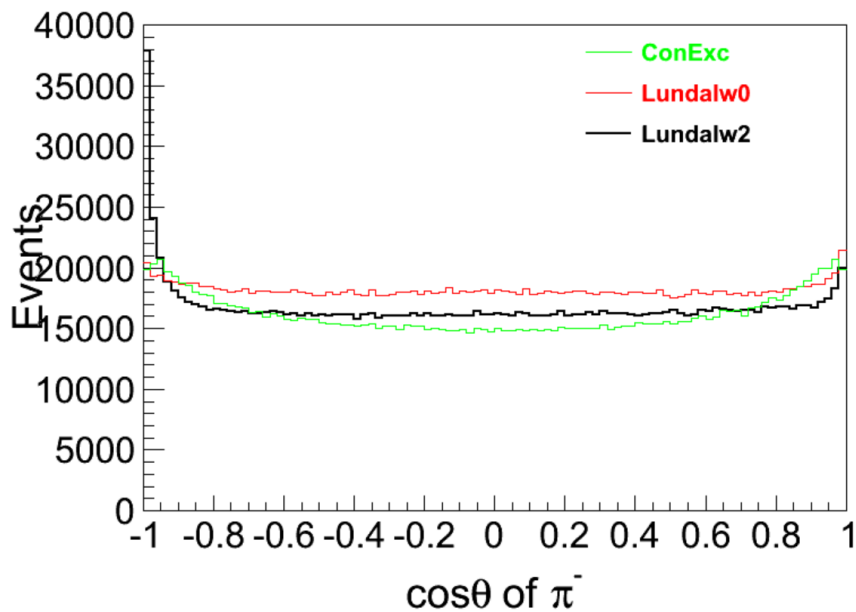
Lundalw0 (Total fit)



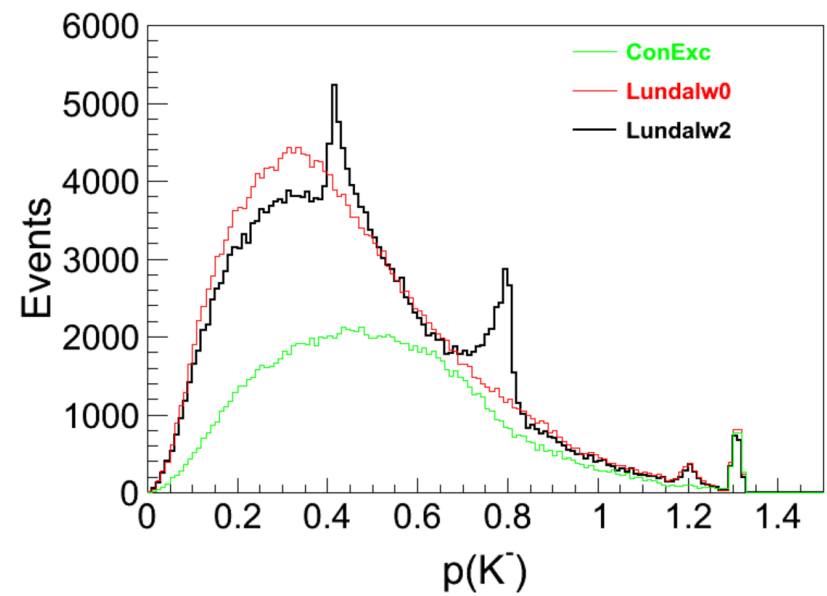
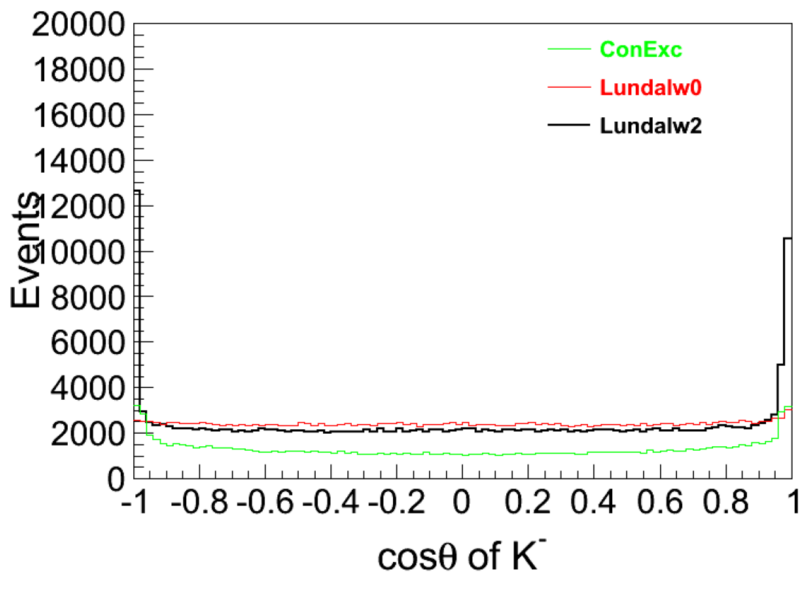
MC truth of π^+



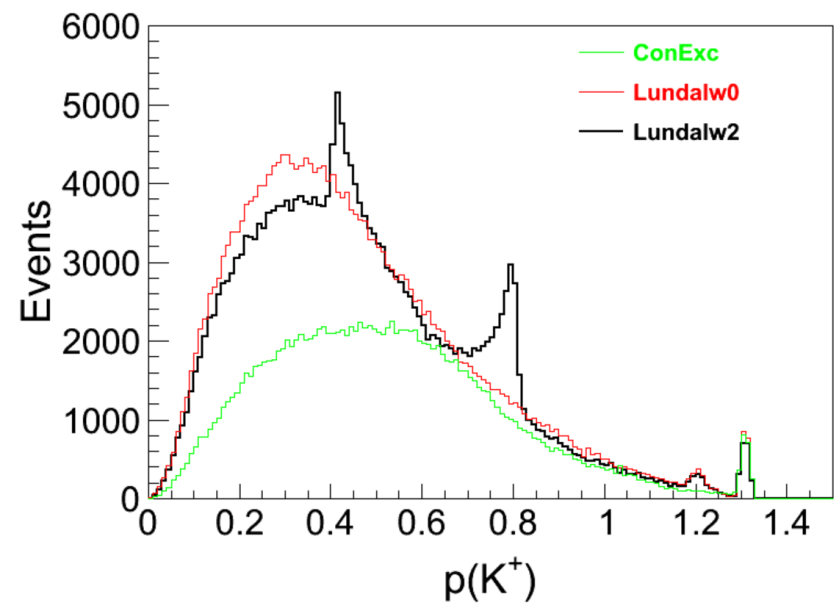
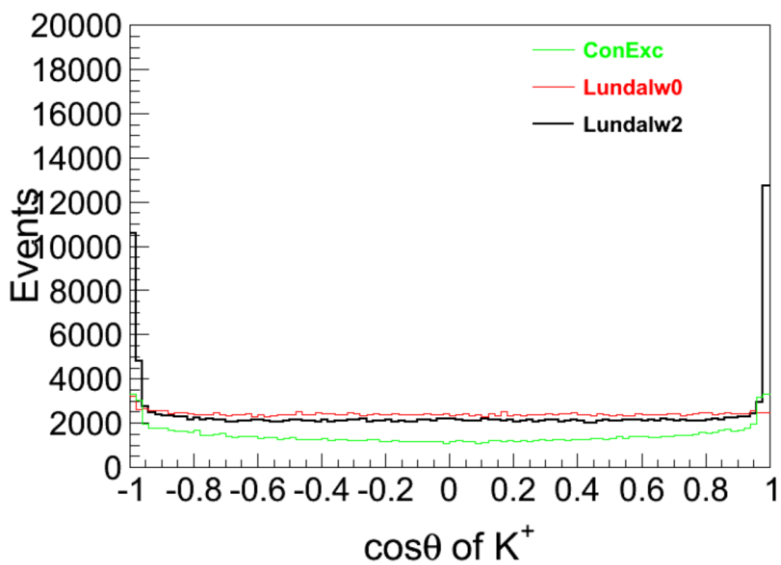
MC truth of π^-



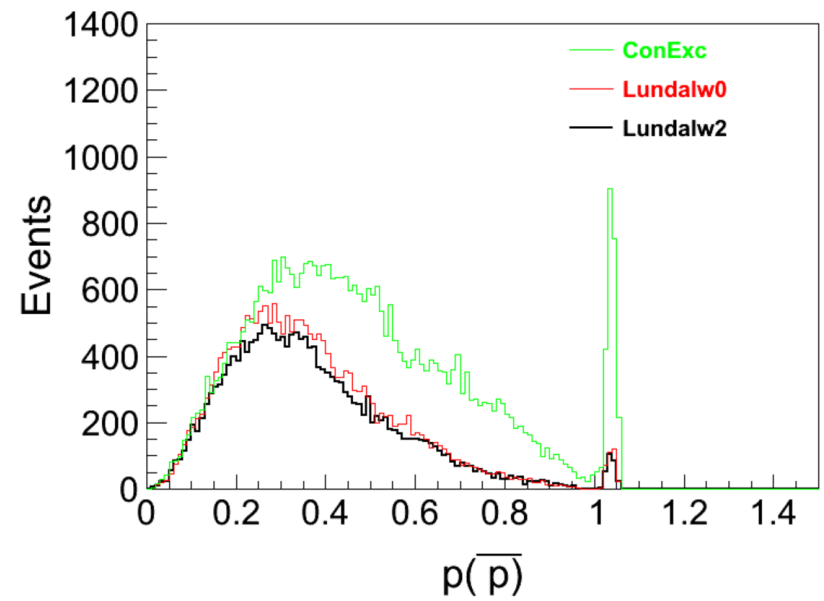
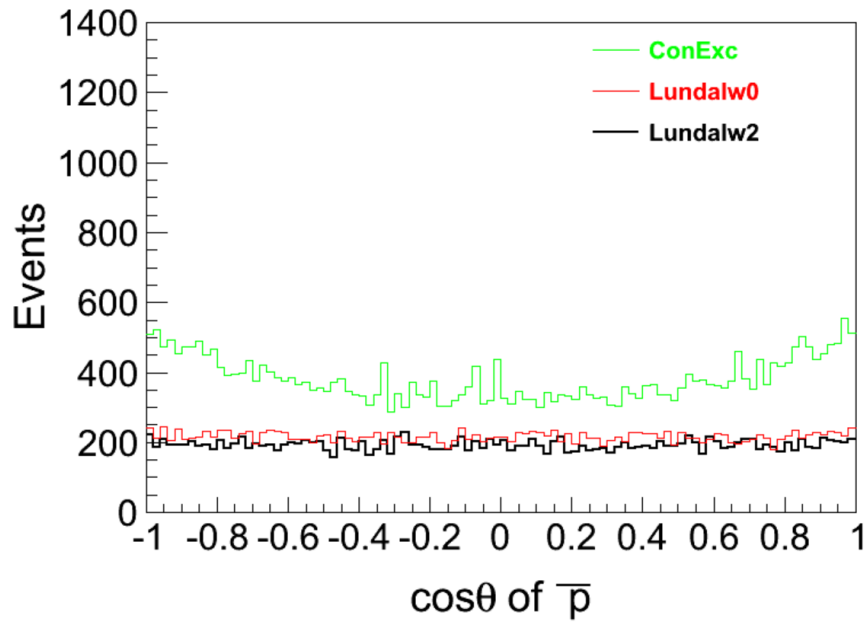
MC truth of K⁻



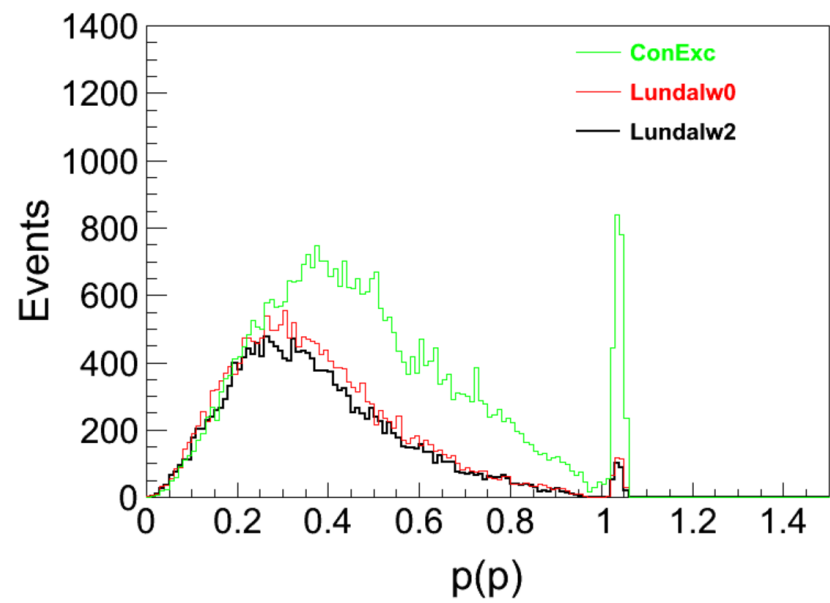
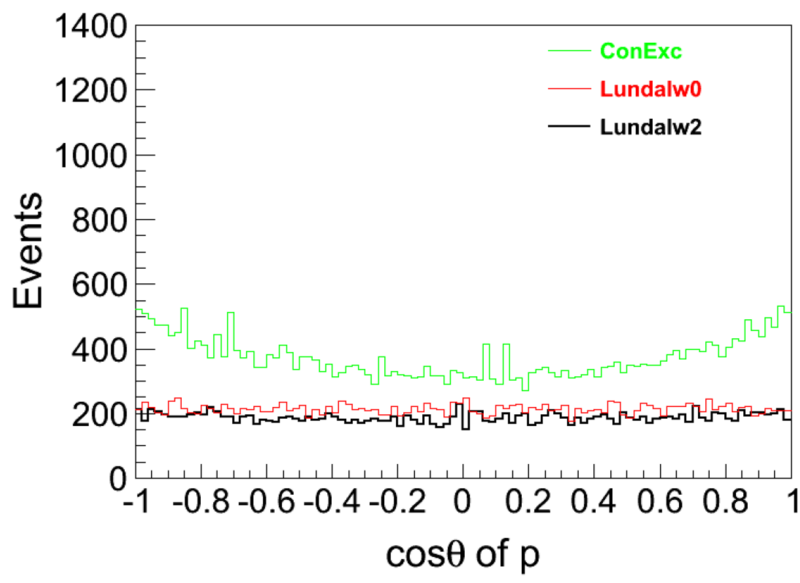
MC truth of K⁺



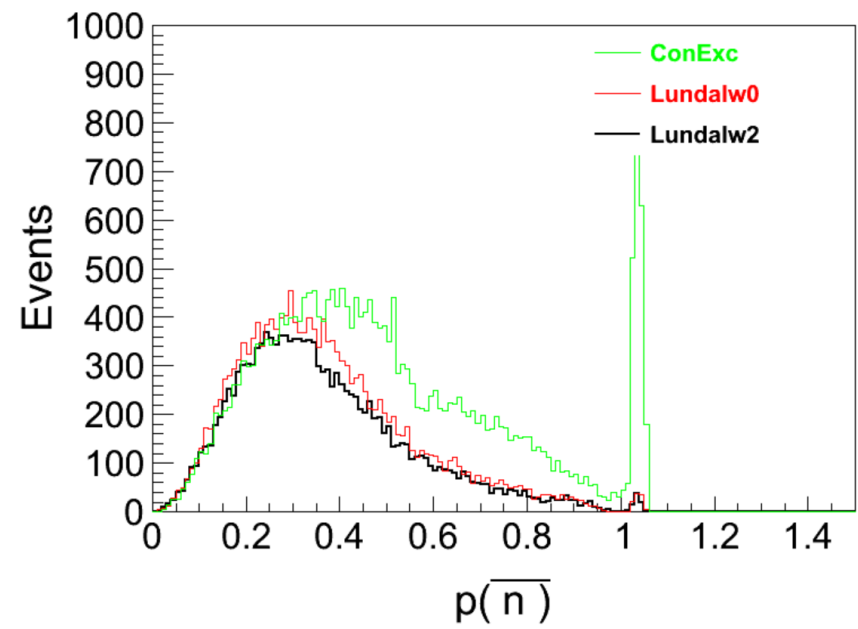
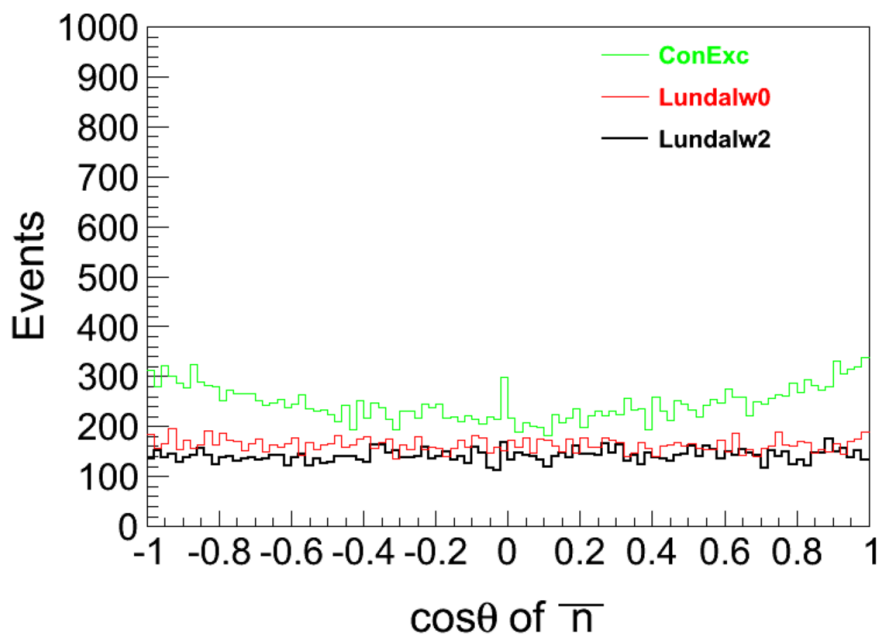
MC truth of anti-proton



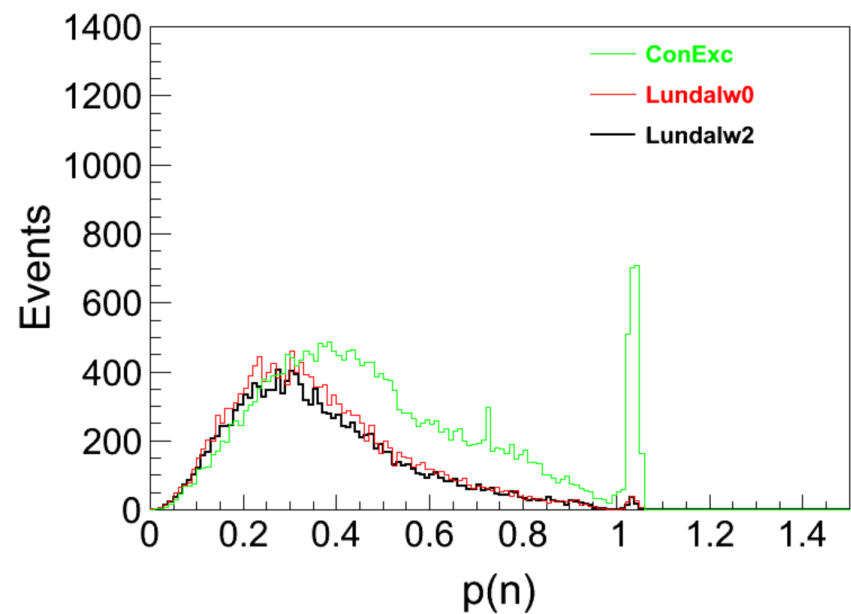
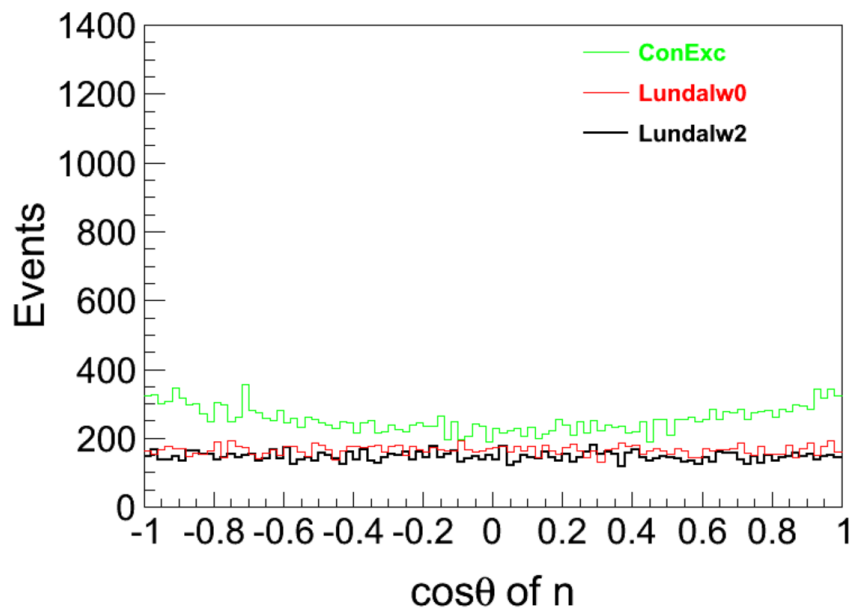
MC truth of proton



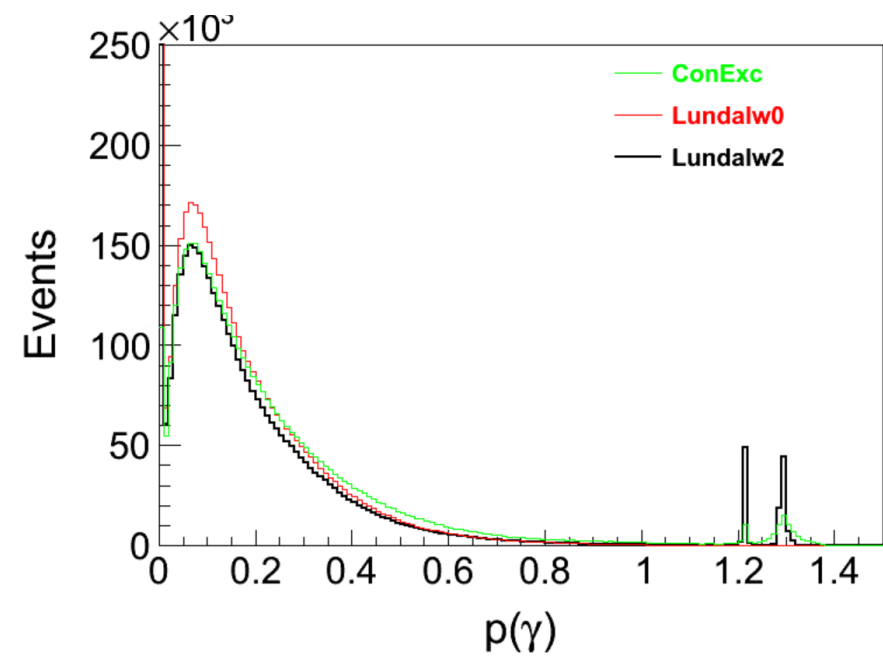
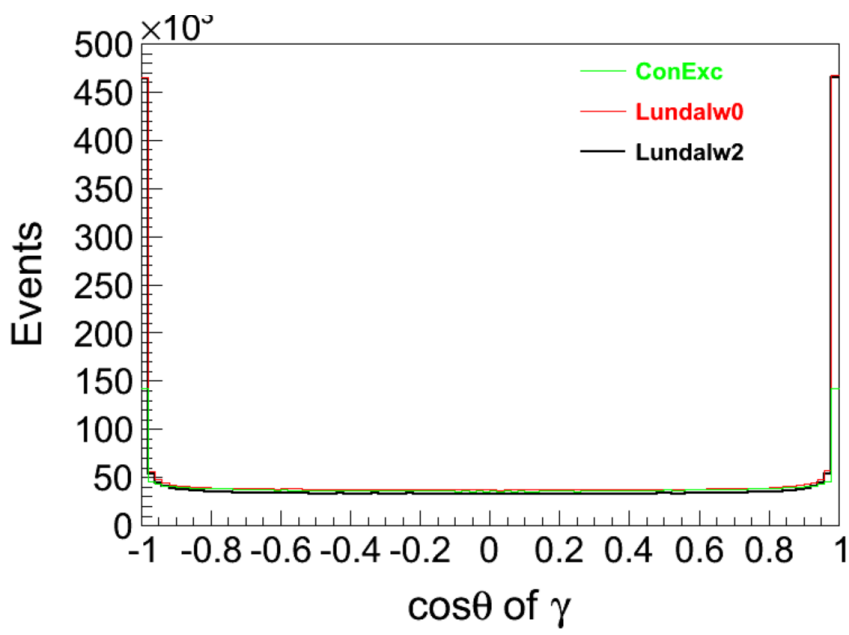
MC truth of anti-neutron

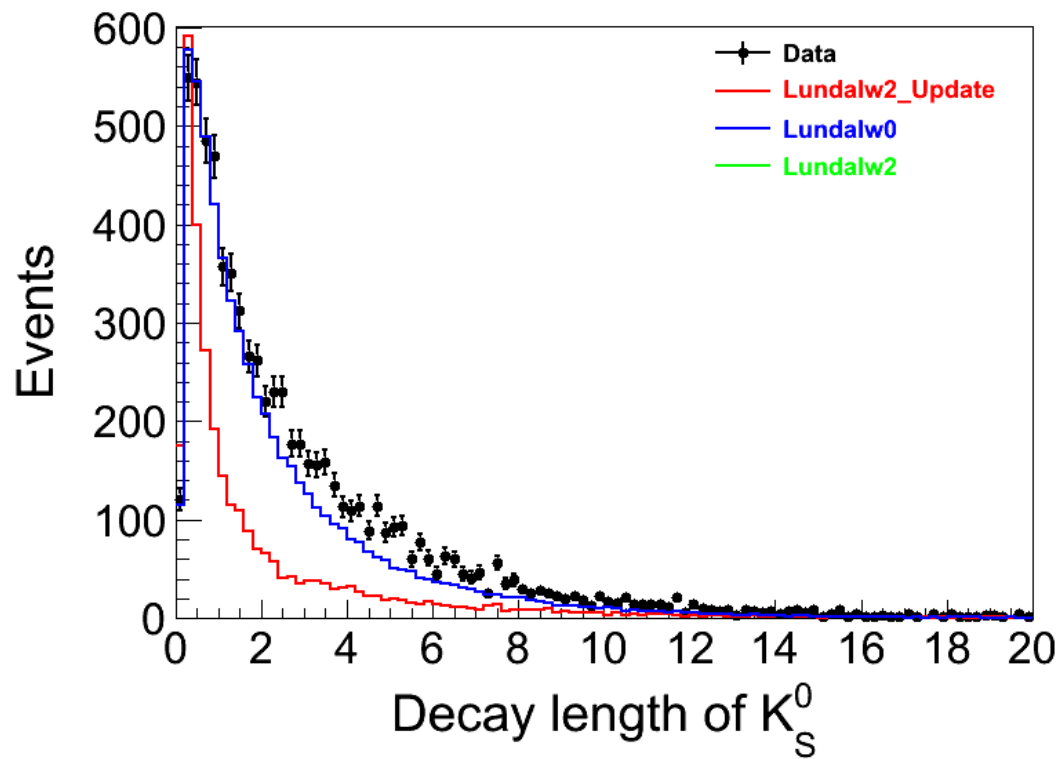


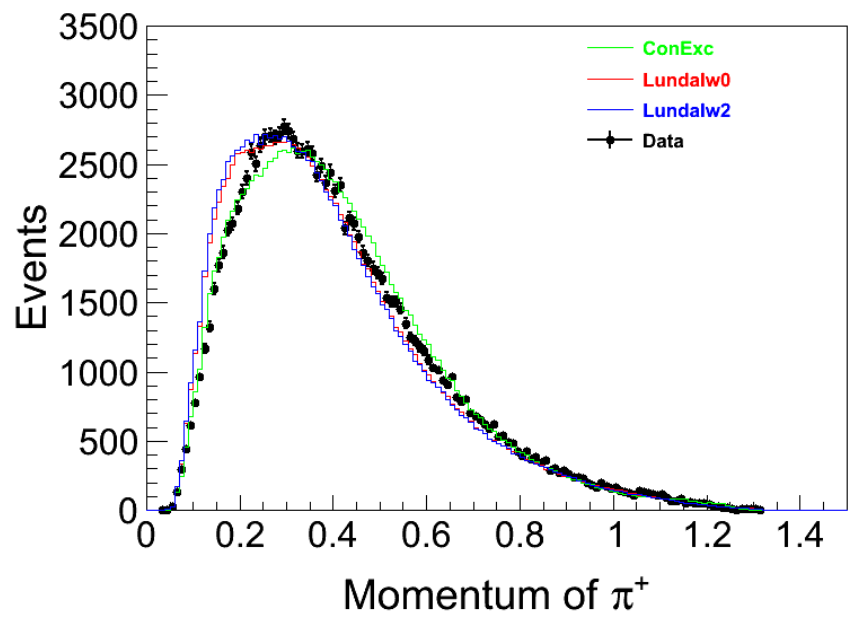
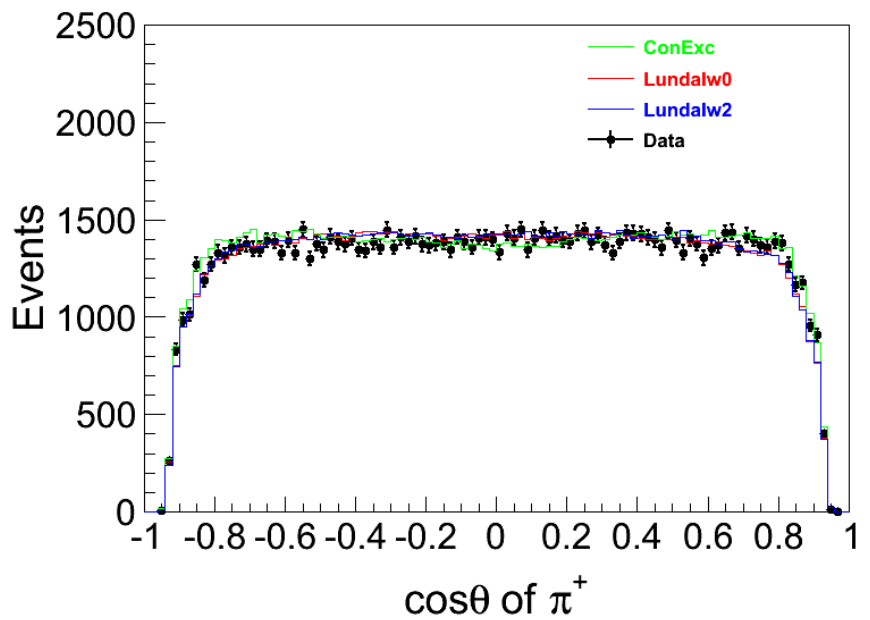
MC truth of neutron

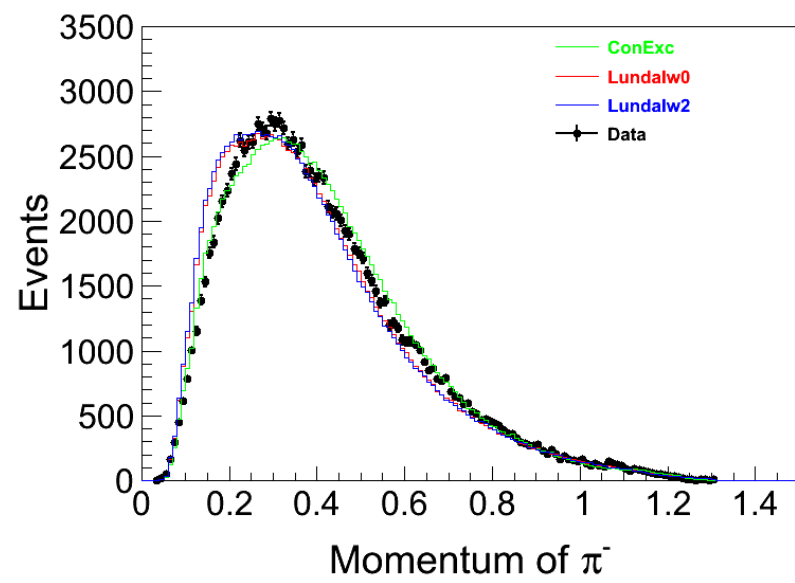
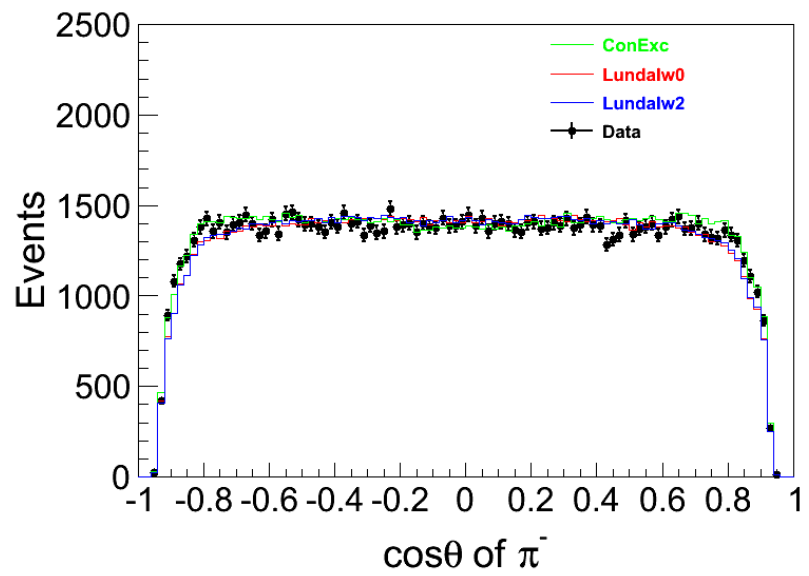


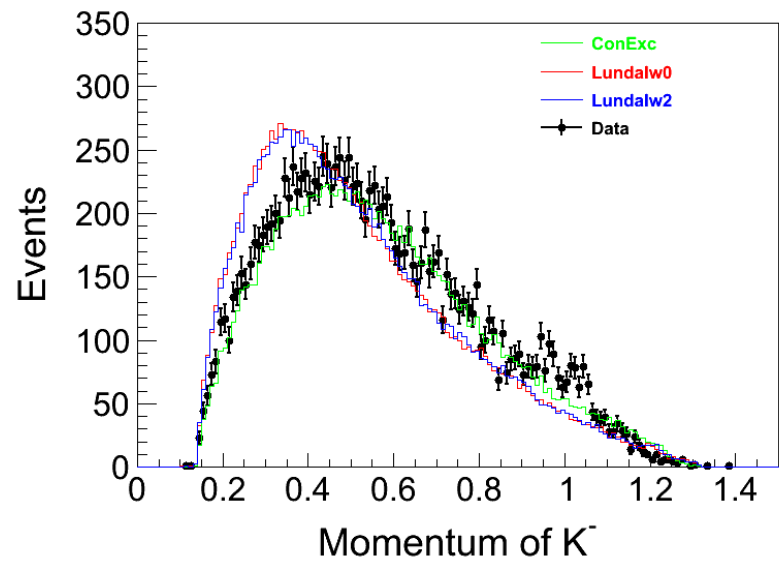
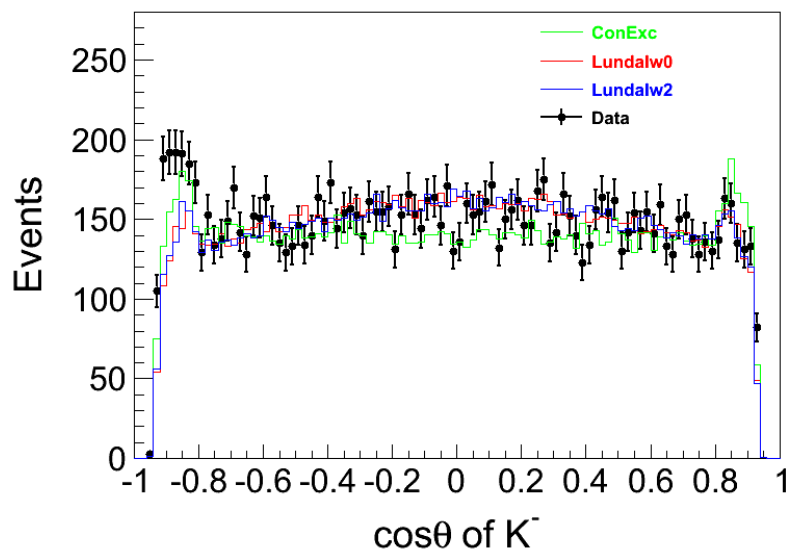
MC truth of gamma

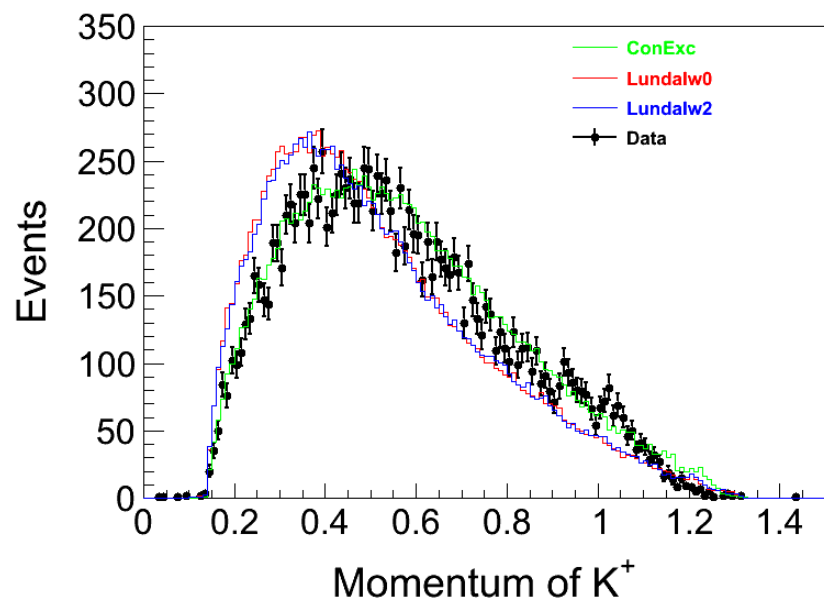
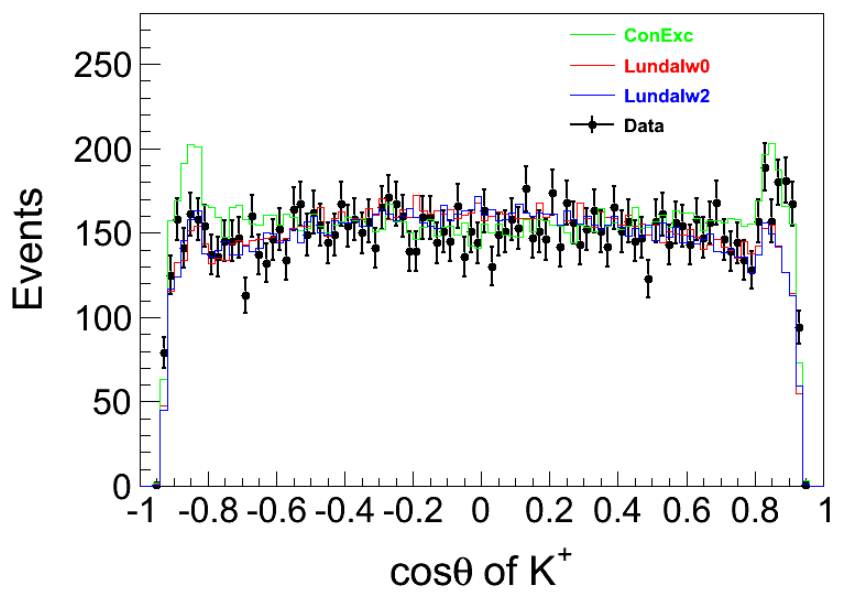












145 **4.2 Bhabha suppression**

146 QED processes like Bhabha and di-mu have large cross section and can pollute interest
147 signal. The tracks of Bhabha events are mainly in the forward directions of e^\pm beams
148 and hit the endcap of the detector, as shown in Fig. 3 and 4. Thus polar angle can be
149 used to veto them with requirement: $\cos\theta_+ < 0.8$ for positive tracks and $\cos\theta_- > -0.8$
150 for negative tracks.

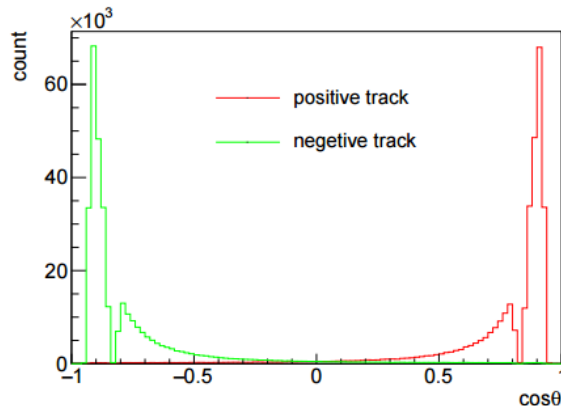
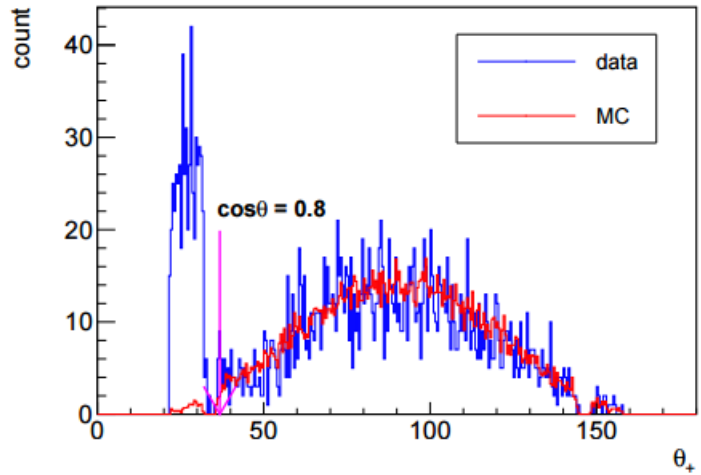
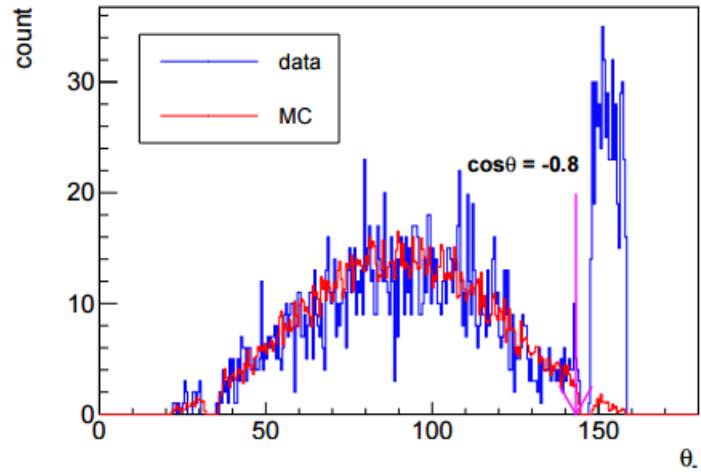


Figure 3: Polar angle distribution of tracking from Bhabha MC at 2.0 GeV. Red line is positive tracks. Green line is negative tracks.

151 After rejecting forward tracks, there are still lots of Bhabha events. Further study
152 shows the ratio of energy deposit in EMC to the momentum of the track (E/p) can be
153 used to separate K^\pm and e^\pm . Plots in Fig. 5 are the E/p spectra of e^\pm and K^\pm showing
154 that most E/p of e^\pm accumulate at 1, while the E/p of K^\pm are far away from 1, indicating
155 E/p can be used to veto Bhabha events. The cut value is optimized via maximizing signal
156 to noise ratio.



a) polar angle of positive charged track



b) polar angle of negative charged track

Figure 4: Polar angle distribution of tracks at 2.0 GeV. Red line is from K^+K^- MC. Blue line is from data. For data, the events are after all events selection criteria except rejecting forward tracks.